

# **Development of Thermal Solutions for Hydrogen Storage in Porous Structures**

Kristoffer Abrahamsen

February 23, 2010



## ABSTRACT

### English

The thermal properties of a new sorption type material used for hydrogen storage are to be measured. The properties are thermal conductivity, specific heat capacity, density, porosity, and permeability. Relevant measurement techniques and principals have been evaluated. Definite propositions for measurements of the specific heat capacity, density, and porosity have been given. For the thermal conductivity and permeability, there have been designed measurement test setups.

A transient method for measurement of thermal diffusivity has been evaluated for one dimensional and radial heat flux. The method has been shown to demand very accurate positioning of the temperature sensors. A steady state measurement method has also been evaluated for radial heat flux. Simulations, error analysis, and real measurements have shown that the steady state method is most reliable.

Darcy's law has been used for development of a principal design of a test rig for permeability.

### Norwegian

De termiske egenskapene til et nytt sorpsjonsmateriale for hydrogenlagring skal måles. De relevante egenskapene er termisk konduktivitet, spesifikk varmekapasitet, tetthet, porøsitet og permabilitet. Det har blitt gjort rede relevante måleteknikker og prinsipper. For spesifikk varmekapasitet, tetthet og porøsitet har det blitt foreslått konkrete målemetoder. For termisk konduktivitet og permabilitet har det blitt designet målerigger.

En transient målemetode for måling av termisk diffusivitet har blitt undersøkt for éndimensjonal og radiell varmefluks. Metoden har vist seg å kreve veldig presis posisjonering av temperatursensorene. En målemetode for stasjonære målinger har også blitt undersøkt for radiell varmefluks. Simuleringer, feilanalyse og målinger har vist at den stasjonære målemetoden er mest pålitelig.

Darcys lov har blitt brukt for å utvikle en prinsipiell design av en målerigg for permeabilitet.





## PREFACE

This project has been written in the period from September to December 2009, it is a part of a research project between NTNU, Max Planck Institut für Metallforschung, and Technische Universität Dresden.

I would like to thank Erling Næss for valuable consultation during this autumn. My work in the laboratory has been significantly easier to perform thanks to Reidar Tellebon, Erling Mikkelsen, Halvor Flatberg, Helge Laukholm, and Erik Langøren who have assisted me with practical problems.

The project has given me many challenges, and I look forward to continue next year.

Trondheim, February 23, 2010

Kristoffer Abrahamsen



# CONTENTS

<b>1. Summary</b>	<b>1</b>
<b>2. Introduction</b>	<b>2</b>
2.1. Background	2
2.2. Project Description	3
 <b>I Relevant Measurement Techniques and Instrumentation</b>	 <b>4</b>
<b>3. Thermal Properties and Physics Relevant for the Metal-Organic Framework</b>	<b>5</b>
3.1. Basis	5
3.2. The Conduction Equation	5
3.3. Fouriers's Law of Heat Conduction	5
3.4. Darcy's Law	6
3.5. The Ideal Gas Law	6
<b>4. Measurement Methods</b>	<b>7</b>
4.1. Basis	7
4.2. Thermal Conductivity	7
4.3. Thermal Diffusivity	7
4.4. Permeability	9
4.5. Density	10
4.6. Specific Heat Capacity	10
4.7. Porosity	10
<b>5. Instrumentation</b>	<b>12</b>
5.1. Basis	12
5.2. Temperature	12
5.3. Pressure	13
5.4. Data Logger	13
5.5. Power Supply	13
 <b>II Principal Designs</b>	 <b>14</b>
<b>6. Thermal Diffusivity - Centered Heater</b>	<b>15</b>
6.1. Basis	15
6.2. Principal Design	15
6.3. Analysis	15
6.4. Cost Estimate	18
6.5. Conclusion	19
<b>7. Thermal Diffusivity - Heater Below</b>	<b>20</b>
7.1. Basis	20
7.2. Principal Design	20
7.3. Analysis	21
7.4. Cost Estimate	22
7.5. Conclusion	22
<b>8. Permeability</b>	<b>23</b>
8.1. Basis	23
8.2. Principal Design	23

8.3. Analysis . . . . .	23
8.4. Cost Estimate . . . . .	24
8.5. Conclusion . . . . .	25
<b>III Completion</b>	<b>26</b>
<b>9. Test Rig for Thermal Conductivity</b>	<b>27</b>
9.1. Basis . . . . .	27
9.2. Experimental Method and Equipment . . . . .	27
9.3. Test and Adjustments . . . . .	27
9.4. Evaluation of Data . . . . .	28
9.5. Measurement Results . . . . .	29
<b>10. Test Rig for Thermal Diffusivity</b>	<b>30</b>
10.1. Basis . . . . .	30
10.2. Choice of Materials and Dimensions . . . . .	30
10.3. Data Reduction . . . . .	31
10.4. Positioning . . . . .	31
10.5. Completion . . . . .	32
<b>11. Closure</b>	<b>33</b>
11.1. Conclusion . . . . .	33
11.2. Further Developments . . . . .	34
<b>IV Appendices</b>	<b>A</b>
<b>A. P&amp;ID</b>	<b>B</b>
A.1. Thermal Diffusivity - Heater Below . . . . .	B
A.2. Thermal Diffusivity - Centered Heater . . . . .	C
<b>B. Measurement Results Radial Rig</b>	<b>D</b>
B.1. 25 November 2009 . . . . .	D
B.2. 1 Desember 2009 . . . . .	F
B.3. 7 Desember 2009 . . . . .	G
<b>C. Dimensioning of Test Rig for Thermal Diffusivity</b>	<b>H</b>
C.1. Basis . . . . .	H
C.2. Case 1 . . . . .	H
C.3. Case 2 . . . . .	J
C.4. Case 3 . . . . .	K
C.5. Case 4 . . . . .	L
<b>D. Measurement of Density</b>	<b>N</b>
D.1. Mettler Toledo AT261 . . . . .	N
<b>E. Measurement of Specific Heat</b>	<b>O</b>
E.1. TGA Q500 . . . . .	O
<b>F. Measurement of Porosity</b>	<b>P</b>
F.1. Beckman Coulter SA 3100 . . . . .	P
<b>Bibliography</b>	<b>Q</b>
<b>Equipment and Material References</b>	<b>R</b>

## LIST OF FIGURES

2.1. Aluminium Foam . . . . .	3
3.1. Porous Media . . . . .	6
4.1. Nodes in One Dimension . . . . .	8
4.2. Radial Nodes . . . . .	8
4.3. Permeability Measurement . . . . .	9
4.4. Calorimeter . . . . .	10
4.5. Porosity Measurement . . . . .	11
5.1. Tube Manometer . . . . .	13
6.1. Principal Design - Centered Heater . . . . .	15
6.2. Temperature Development with Insulated Walls . . . . .	17
6.3. Temperature Profile, Steady State . . . . .	18
7.1. Principal Design - Heater Below . . . . .	20
8.1. Principal Design - Permeability . . . . .	23
8.2. Pressure Drop in the Pipe . . . . .	24
9.1. Measurement Setup . . . . .	27
9.2. Picture of Test Rig with Radial Heater . . . . .	28
9.3. Smoothing of Fluctuations . . . . .	29
10.1. Temperature Distribution . . . . .	30
10.2. Positioning of Thermocouples . . . . .	32
A.1. P&ID - Heater Below . . . . .	B
A.2. P&ID - Centered Heater . . . . .	C
B.1. Temperature and Diffusivity Plot 25 November, $\Delta t = 1s$ - Radial Heater . . . . .	D
B.2. Temperature and Diffusivity Plot 25 November, $\Delta t = 30s$ - Radial Heater . . . . .	E
B.3. Temperature and Conductivity Plot 1 Desember - 1 . . . . .	F
B.4. Temperature and Conductivity Plot 1 Desember - 2 . . . . .	F
B.5. Temperature and Diffusivity Plot 7 Desember, $\Delta t = 30s$ - Radial Heater . . . . .	G
B.6. Temperature and Diffusivity Plot 7 Desember, $\Delta t = 5s$ - Radial Heater . . . . .	G
C.1. Temperature Distribution at $t = 2400s$ , $D_i = 110mm$ . . . . .	I
C.2. Heat Flux at $t = 600s$ , $D_i = 110mm$ . . . . .	I
C.3. Thermal Diffusivity Calculation, $D_i = 110mm$ . . . . .	J
C.4. Heat Flux at $t = 600s$ , $D_i = 60mm$ . . . . .	J
C.5. Thermal Diffusivity Calculation, $D_i = 60mm$ . . . . .	K
C.6. Heat Flux at $t = 600s$ , $D_i = 150mm$ . . . . .	K
C.7. Thermal Diffusivity Calculation, $D_i = 150mm$ . . . . .	L
C.8. Heat Flux at $t = 600s$ , $D_i = 130mm$ . . . . .	L
C.9. Thermal Diffusivity Calculation, $D_i = 130mm$ . . . . .	M
D.1. Mettler AT261 . . . . .	N
E.1. TGA Q500 . . . . .	O

F.1. Beckman Coulter SA 3100 . . . . .	P
--	---

## LIST OF TABLES

3.1. The Relevant Properties . . . . .	5
5.1. Thermocouple Types . . . . .	12
6.1. Test Values . . . . .	16
6.2. Nominal Values and Errors . . . . .	17
6.3. Nominal Values and Errors . . . . .	18
6.4. Cost Estimate - Centered Heater . . . . .	19
7.1. Test Values . . . . .	21
7.2. Nominal Values and Worst Case Error . . . . .	21
7.3. Cost Estimate - Heater Below . . . . .	22
8.1. Nominal Values and Errors . . . . .	25
8.2. Cost Estimate - Permeability Rig . . . . .	25
10.1. Thermal Diffusivity in Tabular Form . . . . .	31
B.1. Measurement Setup 25 November - Radial Heater . . . . .	D
B.2. Measurement Setup 1 Desember - Radial Heater . . . . .	F
B.3. Measurement Setup 25 November - Radial Heater . . . . .	G
C.1. Simulation Input Data . . . . .	H
C.2. Simulation Input Data . . . . .	J
C.3. Simulation Input Data . . . . .	K
C.4. Simulation Input Data . . . . .	L

# NOMENCLATURE

## Abbreviations

EU	European Union
NTNU	The Norwegian University of Science and Technology
MOF	Metal-Organic Framework
PFTE	Polytetrafluoroethylene, Teflon
PMMA	Polymethyl-methacrylate, Plexiglass
PRT	Platinum Resistance Thermometer
P&ID	Piping and Instrumentation Diagram
TFDA	Transient Finite Difference Approach

## Symbols

$\alpha$	Thermal Diffusivity [ $\frac{m^2}{s}$ ]	$\Delta\epsilon_{st}$	Statistical Error
$\Delta\epsilon_{wc}$	Worst Case Error	$\kappa$	Permeability [ $m^2$ ]
$\Delta E$	Energy Difference [ $J$ ]	$\Delta x$	Length Between Nodes [ $m$ ]
$\Delta t$	Time Step [ $s$ ]	$\Delta T$	Temperature Permissiveness [ $K$ ]
$\Delta r$	Radial Position Permissiveness [ $m$ ]	$\Delta(\Delta t)$	Time Step Permissiveness [ $s$ ]
$\Delta\dot{Q}$	Heat Permissiveness [ $W$ ]	$\Delta h$	Height Permissiveness [ $m$ ]
$\Delta(\Delta x)$	One Dimensional Position Permissiveness [ $m$ ]	$\Delta P$	Pressure Difference Permissiveness [ $Pa$ ]
$\Delta u$	Velocity Permissiveness [ $\frac{m}{s}$ ]	$\Delta\mu$	Dynamic Viscosity Permissiveness [ $\frac{kg}{ms}$ ]
$\Delta L$	Length Permissiveness [ $m$ ]	$\rho$	Density [ $\frac{kg}{m^3}$ ]
$c_v$	Specific Heat Capacity, constant volume [ $\frac{J}{kgK}$ ]	$\mu$	Dynamic Viscosity [ $\frac{kg}{ms}$ ]
$c_p$	Specific Heat Capacity, constant pressure [ $\frac{J}{kgK}$ ]	$\Phi$	Porosity [1]
$k$	Thermal Conductivity [ $\frac{W}{mK}$ ]	$T$	Temperature [ $K$ ]
$\dot{Q}$	Heat Transfer Rate [ $W$ ]	$A$	Area [ $m^2$ ]
$x$	One Dimensional Length [ $m$ ]	$r$	Radial Length [ $m$ ]
$h$	Height [ $m$ ]	$V$	Volume [ $m^3$ ]
$u$	Velocity [ $\frac{m}{s}$ ]	$P$	Pressure [ $Pa$ ]
$L$	Length [ $m$ ]	$m$	Mass [ $kg$ ]
$R$	Gas Constant [ $\frac{J}{kgK}$ ]	$\dot{Q}$	Volumetric Flow Rate [ $\frac{m^3}{s}$ ]
$I$	Current [ $A$ ]	$V$	Volt [ $V$ ]
$D$	Diameter [ $m$ ]	$g$	Gravitational Acceleration [ $\frac{m}{s^2}$ ]

## Superscripts and Subscripts

$i$	Time Step	$_{gen}$	Generate	$_{ref}$	Reference Case
$m$	Node Number	$_{cond}$	Conduction	$_{\beta}$	Void Fraction
$f$	Fluid	$_{s}$	Sample	$_{\sigma}$	Solid Fraction



## SUMMARY

The thermal properties of a new sorption type material used for hydrogen storage are to be measured. In order to do this, relevant measurement techniques and principles must be found. The relevant properties are the thermal conductivity, specific heat capacity, density, porosity, and permeability.

A literature study has been done to find suitable measurement methods, and the physical laws behind the methods have been reviewed. Definite propositions for measurements of the specific heat capacity, density, and porosity have been given. For the thermal conductivity and permeability, there have been designed measurement test setups.

Two test setups for measurement of thermal diffusivity have been designed and analyzed. The principal difference between the two rigs is the placing of the heating elements. Depending on if the heating element is placed underneath or in the center of the specimen, the heat will transfer one-dimensionally or radially, respectively. A transient measurement method have been examined in addition to Fourier's law of heat conduction for steady state measurements. The thermal conductivity can be calculated from the diffusivity when the density and specific heat are known.

For the permeability, a principal design has been developed where Darcy's law is applied. The influence of wall friction have not been considered.

Relevant instrumentation for the test rigs have been reviewed and rough cost estimates have been worked out. The possible sources of errors have been evaluated on all test rigs to find the needed accuracies of the sensors and their positioning. MAPLE has been used to manage advanced differentiate operations. The positioning of the temperature sensors has been pointed out to be the most crucial factor for thermal conductivity and diffusivity measurements. The permeability rig has been shown to deliver proper results with the assumed inaccuracies.

Simulations have been done in COMSOL to test the different measuring methods. The simulated data has been exported to MATLAB for further evaluation and model testing.

Thermal conductivity and diffusivity measurements have been performed on a rig with centered heater in the laboratory. Together with the simulations and error analysis, the measurements have shown that steady state measurements with Fourier's law are able to deliver more accurate results than the transient method.

## INTRODUCTION

### **2.1** Background

Over 98 % of all today's vehicles in the EU use fossil fuel as energy carrier [6], the high energy density makes the fuel superior compared to other alternatives. However, the supply of fossil fuel will end and is harmful for the environment; there is need for a replacement.

Hydrogen is a possible energy storage medium for the transport sector where high energy density can be obtained. Combustion of hydrogen is environmentally friendly as the only product is water. There is nevertheless still some challenges to be faced regarding storage; the low density of hydrogen under atmospheric pressure and ambient temperature necessitates the need to develop an efficient storage method. For instance, a light duty vehicle requires between 4 to 10 kilograms of hydrogen to attain a range around 480km, not much in a mass perspective, but when considering that the specific volume at ambient conditions is around  $11.9 \frac{m^3}{kg}$  [1] the numbers are self explanatory.

Today, compressed gas are the preferred method for onboard storage. To obtain a decent energy density it is necessary to compress the gas in the order of 350 to 700 bar. The high pressure carries along safety concerns in the occurrence of an accident and a great energy demand for compression. Another way of storage is liquid tanks which need insulation and a refrigeration unit to avoid evaporation. Hydrogen in liquid form has lower energy content in volume basis than regular fuel which results in bigger storage tanks. [4, page 15-16]

None of today's storage methods meet the standards imposed by the United States Department of Energy [2] and must therefore be improved. At the same time, other technologies are under research and development. An alternative method is to store hydrogen in solid state, this can be done with adsorbents where the hydrogen attaches to a surface of a solid. Sorption type materials are characterized by high porosity and surface area.

NTNU participates in a development project of so-called Metal-Organic Framework (MOF) together with Max Planck Institut für Metallforschung and Technische Universität Dresden, both located in Germany. The MOF is a sorption type material intended for hydrogen storage. Research have shown that the thermal effects during filling and discharging have a great influence on the utilization of the storage system. The thermal properties of the MOF need to be characterized for further investigation.

### 2.2 Project Description

The purpose of this project is to give an account for relevant measurement techniques and principles of the MOF's thermal properties. The properties to be examined are the thermal conductivity, specific heat capacity, density, porosity, and permeability.

Definite suggestions of ways to measure the properties will be given based on the presented measurement techniques and principles. The main focus of this report has however been to develop a test setup for measurement of thermal diffusivity by using a transient method. The thermal conductivity can be calculated from the thermal diffusivity when the specific heat and density are known.

The MOF will be attached to a foam of aluminium. A picture of the foam is shown in figure 2.1, the foam is also characterized by a high surface area. The thermal properties of the foam will not be investigated.



Figure 2.1.: Aluminium Foam

---

---

PART I

---

Relevant Measurement Techniques  
and Instrumentation

## THERMAL PROPERTIES AND PHYSICS RELEVANT FOR THE METAL-ORGANIC FRAMEWORK

### 3.1 Basis

This chapter reviews the properties and physical laws that will be used in the report. All of the properties are intended to be measured. The following properties are of relevance:

Property	Notation	Unit	Description
Thermal Conductivity	$k$	$\frac{W}{mK}$	The ability of a material to transfer heat.
Specific Heat Capacity	$c_p$	$\frac{J}{kgK}$	The energy required to raise the temperature of a unit mass of a material one degree under constant pressure.
Density	$\rho$	$\frac{kg}{m^3}$	The mass per unit volume.
Porosity	$\Phi$	[1]	A measure of the void fraction of a material.
Permeability	$\kappa$	$m^2$	A measure of the ability for a fluid to flow through the material.
Thermal Diffusivity	$\alpha$	$\frac{m^2}{s}$	A measure on how fast heat diffuses through a material.

Table 3.1.: The Relevant Properties

### 3.2 The Conduction Equation

Conduction is transfer of thermal energy between molecules due to a temperature gradient.

$$\frac{1}{\alpha} \frac{\partial T}{\partial t} = \nabla^2 T \quad (3.1)$$

### 3.3 Fouriers's Law of Heat Conduction

Fourier's law is a steady state solution of the conduction equation.

*One-Dimensional*

$$\dot{Q}_{cond} = -kA \frac{dT}{dx} \quad (3.2)$$

Where  $A$  is the cross sectional area.

*Radial*

$$\dot{Q}_{cond} = -kA(r) \frac{dT}{dr} \quad (3.3)$$

Where  $A(r) = 2\pi rh$ .

#### 3.4 Darcy's Law

Consider a porous media consisting of two phases as illustrated in figure 3.1. The porosity is simply the volume fraction of the void space in the control volume.

$$\Phi = \frac{V_\beta}{V_\sigma} \quad (3.4)$$

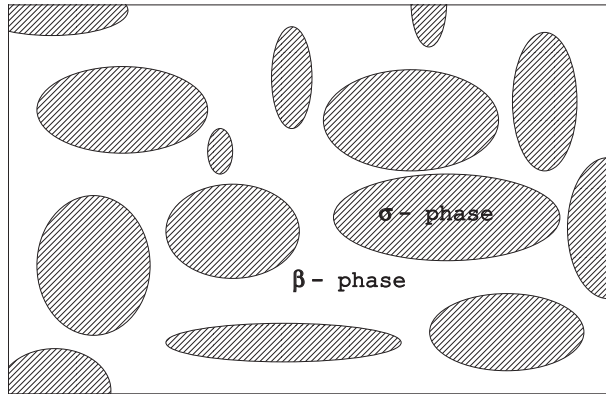


Figure 3.1.: Porous Media

Darcy's Law [7]:

$$\langle \mathbf{u}_\beta \rangle = -\frac{\kappa}{\mu_\beta} \left[ \nabla \langle P_\beta \rangle^\beta - \rho_\beta \mathbf{g} \right] \quad (3.5)$$

Where  $\mathbf{u}_\beta$  is the velocity and  $\mu_\beta$  the viscosity of a fluid flowing through the porous media. The notation  $\langle \rangle$  is used for phase average, and  $\langle \rangle^\beta$  for intrinsic phase average, see equation 3.6.

$$\langle \mathbf{u}_\beta \rangle = \frac{1}{V_\beta + V_\sigma} \int_{V_\beta} \mathbf{u}_\beta dV, \quad \langle \mathbf{u}_\beta \rangle^\beta = \frac{1}{V_\beta} \int_{V_\beta} \mathbf{u}_\beta dV, \quad (3.6)$$

#### 3.5 The Ideal Gas Law

The ideal gas law is the equation of state for an ideal gas.

$$PV = mRT \quad (3.7)$$

## MEASUREMENT METHODS

### **4.1** Basis

This chapter will use the laws introduced in chapter 3 to formulate mathematical expressions for the relevant properties. In addition, some common measuring principles will be introduced.

### **4.2** Thermal Conductivity

The thermal conductivity can be calculated from Fourier's law of heat conduction.

$$k = -\frac{\dot{Q}_{cond}}{A} \frac{dx}{dT} \quad (4.1)$$

In principal, this is a straight forward way to measure the conductivity. However, it can be very time consuming as the temperature profile has to reach steady state. The calculated conductivity will be at an average of the temperature difference.

The conductivity can also be measured through thermal diffusivity if the density and specific heat are known:

$$k = \alpha \rho c_p \quad (4.2)$$

### **4.3** Thermal Diffusivity

#### *4.3.1. Transient Finite Difference Approach (TFDA)*

Consider a volume of any kind exposed for transient heat conduction. The energy balance can be written as [1, Chapter 5]:

$$\sum_{Allsides} \dot{Q} + \dot{E}_{gen} = \frac{\Delta E}{\Delta t} \quad (4.3)$$

Where  $\dot{E}_{gen}$  is the generated energy in the volume, and  $\frac{\Delta E}{\Delta t}$  is the change of energy in the control volume per time step.

#### *One-Dimensional Heat Conduction*

For one-dimensional heat conduction with no heat generation in the control volume, equation 4.3 can be rewritten as:

$$kA \frac{T_{m-1}^i - T_m^i}{\Delta x} + kA \frac{T_{m+1}^i - T_m^i}{\Delta x} = \rho A \Delta x c_p \frac{T_m^{i+1} - T_m^i}{\Delta t} \quad (4.4)$$

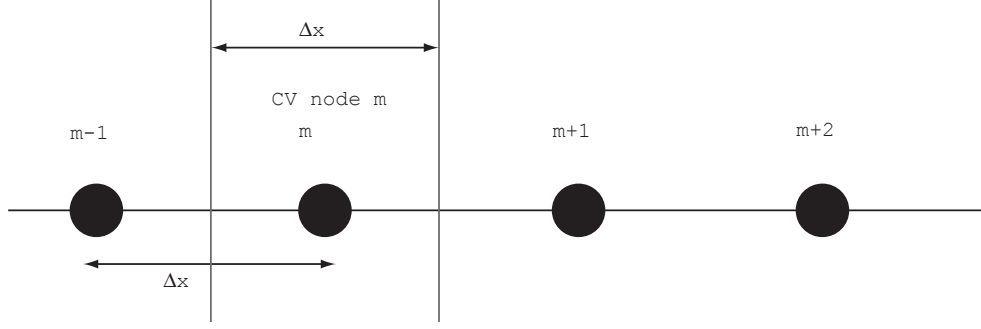


Figure 4.1.: Nodes in One Dimension

Where  $i$  denotes the time step, and  $m$  denotes the node number. The area  $A$  can be cancelled and the thermal diffusivity  $\alpha = \frac{k}{\rho c_p}$  induced:

$$T_{m-1}^i - 2T_m^i + T_{m+1}^i = \frac{\Delta x^2}{\alpha \Delta t} (T_m^{i+1} - T_m^i) \quad (4.5)$$

The thermal diffusivity can be calculated from the following equation:

$$\alpha = \frac{\Delta x^2}{\Delta t} \frac{T_m^{i+1} - T_m^i}{T_{m-1}^i - 2T_m^i + T_{m+1}^i} \quad (4.6)$$

#### Radial Heat Conduction

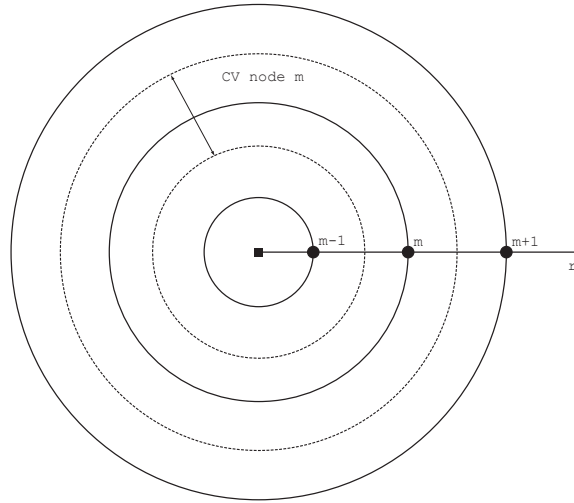


Figure 4.2.: Radial Nodes

Radial heat conduction with no heat generation in the control volume from equation 4.3:

$$\frac{2(T_{m-1}^i - T_m^i)}{\ln(\frac{r_m}{r_{m-1}})} + \frac{2(T_{m+1}^i - T_m^i)}{\ln(\frac{r_{m+1}}{r_m})} = \frac{1}{\alpha} \frac{T_m^{i+1} - T_m^i}{\Delta t} \cdot \frac{V}{h} \quad (4.7)$$

Where  $\frac{V}{h} = \frac{\pi}{4} (r_{m+1}^2 + 2(r_m r_{m+1} - r_{m-1} r_m) - r_{m-1}^2)$ . This is the control volume of each node, illustrated in figure 4.2.

$$T_m^{i+1} = 2\alpha \Delta t \frac{h}{V} \left[ \frac{(T_{m-1}^i - T_m^i)}{\ln(\frac{r_m}{r_{m-1}})} + \frac{(T_{m+1}^i - T_m^i)}{\ln(\frac{r_{m+1}}{r_m})} \right] + T_m^i \quad (4.8)$$



The thermal diffusivity can be calculated from the following equation:

$$\alpha = \frac{T_m^{i+1} - T_m^i}{\frac{8\Delta t}{\pi(r_{m-1}^2 + 2(r_m r_{m+1} - r_{m-1} r_m) - r_{m-1}^2)} \left[ \frac{T_{m-1}^{i+1} - T_m^{i+1}}{\ln(\frac{r_m}{r_{m-1}})} + \frac{T_{m+1}^{i+1} - T_m^{i+1}}{\ln(\frac{r_{m+1}}{r_m})} \right]} \quad (4.9)$$

*Explicit or Implicit?*

The equations in this section can be formulated both explicit and implicit, it depends on the time derivative which can be in forward or backward difference form. In other words, it depends on which time step the heat contribution between the nodes is evaluated; explicit:  $\sum \dot{Q}^i$ , implicit:  $\sum \dot{Q}^{i+1}$ . When the temperatures are to be measured, there are two ways to calculate the thermal diffusivity.

#### 4.3.2. Radial Solution of Conduction Equation

The conduction equation written in cylindrical coordinates:

$$\frac{1}{r} \frac{\partial}{\partial r} \left( r \frac{\partial T}{\partial r} \right) + \frac{1}{r^2} \frac{\partial^2 T}{\partial \theta^2} + \frac{\partial^2 T}{\partial z^2} = \frac{1}{\alpha} \frac{\partial T}{\partial t} \quad (4.10)$$

The heat is assumed to only spread radially:

$$\frac{1}{r} \frac{\partial}{\partial r} \left( r \frac{\partial T}{\partial r} \right) = \frac{1}{\alpha} \frac{\partial T}{\partial t} \quad (4.11)$$

The equation is solved in [3, Section 11.5.2]:

$$T(r, t) = A_1 (r^2 + 4\alpha t) + A_2 \quad (4.12)$$

Where  $A_1$  and  $A_2$  are constants. The thermal diffusivity can be found by measuring the time it takes for the temperature at  $r_1$  to reach  $r_2$ ,  $T(r_1, t_1) = T(r_2, t_2)$ .

$$\alpha = \frac{r_2^2 - r_1^2}{4\Delta t} \quad (4.13)$$

#### 4.4 Permeability

The permeability can be calculated from Darcy's Law.

$$\kappa = - \frac{\langle \mathbf{u}_\beta \rangle \mu_\beta}{\nabla \langle p_\beta \rangle^\beta - \rho_\beta \mathbf{g}} \quad (4.14)$$

Figure 4.3 illustrates a horizontal case where fluid flows through the porous media.

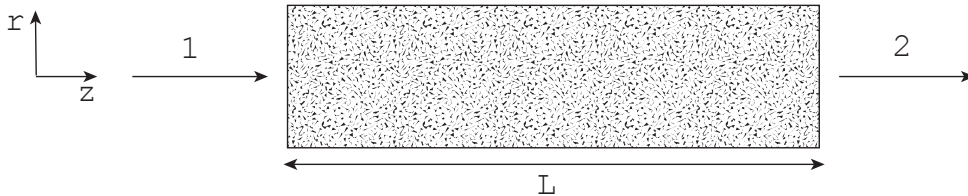


Figure 4.3.: Permeability Measurement

$$\kappa = \frac{u_z \mu L}{P_2 - P_1} \quad (4.15)$$

The permeability is obtained by measuring the pressure drop and the superficial velocity over the sample.

#### 4.5 Density

The density can easily be measured; all needed is a container with a known volume and a weight. The measurements must be done under varied temperatures and pressures to examine the compressibility of the material.

$$\rho = \frac{m_{sample}}{V_{sample}} \quad (4.16)$$

Measurement of density can be done at the department of energy and process engineering at NTNU, see appendix D.

#### 4.6 Specific Heat Capacity

The specific heat capacity is a measure of the energy required to raise the temperature of a unit mass one degree. The measurement can be done under either constant pressure or volume; hence, the notation  $c_p$  and  $c_v$ . The specific heat capacity under constant pressure is considered in this section. The relation between the specific heat under constant pressure and constant volume is:

$$C_p - C_v = R \quad (4.17)$$

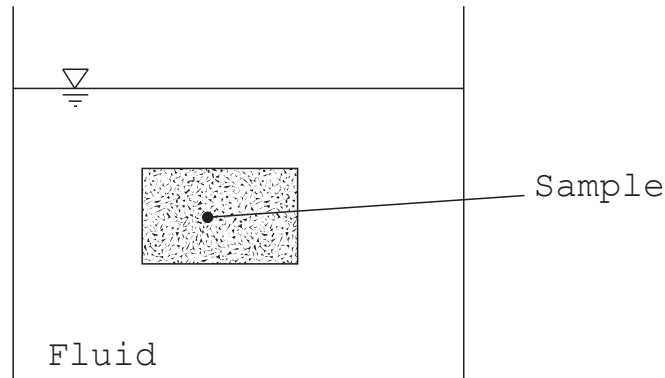


Figure 4.4.: Calorimeter

The change in temperature when a sample is put into a fluid of different temperature can be used to measure the specific heat. If the container is assumed to be insulated, the heat will only transfer between the sample and fluid.

$$\delta Q = (mc_p dT)_f = (mc_p dT)_s \quad (4.18)$$

Where  $f$  denotes the fluid in the container, and  $s$  the sample to be measured.

$$c_{p,s} = c_{p,f} \frac{m_f}{m_s} \frac{T_{0,f} - T_{end}}{T_{0,s} - T_{end}} \quad (4.19)$$

The specific heat is obtained by measuring the initial temperatures of the fluid and sample, and measure the balance temperature,  $T_{end}$ .

Measurement of specific heat can be done at the department of chemical engineering at NTNU, see appendix E.

#### 4.7 Porosity

The porosity of a material can be measured in a vacuum tank.

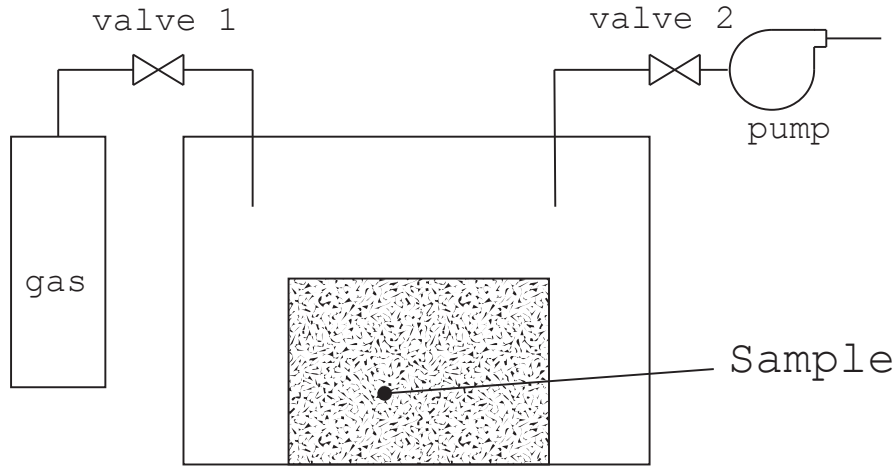


Figure 4.5.: Porosity Measurement

First, a reference case with an empty tank is needed; figure 4.5 illustrates how a pump can be used to create vacuum in the tank. After having reached vacuum, a fixed amount of gas is injected through the other valve and the pressure and temperature is measured. The ideal gas law gives us:

$$pV = mRT \quad (4.20)$$

Where  $R$  is the gas constant and  $m$  the mass of the gas. The volume for the reference case,  $V_{ref}$ , is calculated.

Secondly, the same procedure is followed, but now with the sample inside the tank.  $mR$  is constant for both cases, and the ideal gas law is used to calculate the new volume of the gas:

$$V = \frac{T}{p} \left( \frac{pV}{T} \right)_{ref} \quad (4.21)$$

The volume of the  $\sigma$ -phase is:

$$V_{\sigma} = V_{ref} - V \quad (4.22)$$

The total volume of the sample is known; hence, the volume of the  $\beta$ -phase can be calculated:

$$V_{\beta} = V_{sample} - V_{\sigma} \quad (4.23)$$

Finally, the porosity can be calculated:

$$\Phi = \frac{V_{\beta}}{V_{\sigma}} \quad (4.24)$$

Measurement of porosity can be done at the department of chemical engineering at NTNU, see appendix F.

## INSTRUMENTATION

### **5.1** Basis

This chapter evaluates relevant measurement instrumentation that is considered to be used in the test rigs for thermal diffusivity and permeability.

### **5.2** Temperature

It is important to keep in mind that the test rigs will have relatively small dimensions under the consideration of what kind of thermometers to use. The sensors need to be as small as possible; on the other hand, the accuracy of the measurements is important.

Two main types are considered: thermocouples and resistance thermometers.

#### *5.2.1. Thermocouple Thermometer*

A thermocouple consists of two wires connected in junction which is the temperature measuring point. The wires consist of different materials and produce voltage related to temperature difference. There are many possible material combinations for the wires; as a result, there has been developed a standardization as shown in table 5.1 [3, Section 3.3]:

Type	Temperature Range [°C]		
B	0	-	1820
E	-270	-	1000
J	-210	-	1200
K	-270	-	1372
R	-50	-	1767
S	-50	-	1767
T	-270	-	400

Table 5.1.: Thermocouple Types

The test rig is intended to operate between  $-200^{\circ}\text{C}$  and  $300^{\circ}\text{C}$  which makes several relevant thermocouple types relevant. However, type T is the proper choice because it produces most voltage in the dedicated range [23].

The accuracy of thermocouples varies along with temperature and type, in general it is difficult to achieve a higher accuracy than  $\pm 0.05\text{K}$ . Thermocouples with diameter of  $0.25\text{mm}$  are commercially available.

#### 5.2.2. Resistance Thermometer

Variations in temperature changes the electrical resistance in some materials. This applies for platinum which is the most common material for this purpose. Resistance thermometers are often referred to as platinum resistance thermometers, or PRTs.

PRTs have high accuracy and are stable over time. On the other hand, they have a longer response time and a shorter temperature range than thermocouples. They also tend to be bigger which is a major drawback for the test rig. The most common PRT, PT100, tends to be very expensive for diameters under 1mm.

### 5.3 Pressure

The pressure drop over the permeability rig can be measured with an inclined tube manometer which shows the pressure difference between two points. To obtain higher accuracy, it is smart to incline the tube so the height difference stretches over a longer length. This method is preferable compared to the use of two pressure sensors that must be precisely calibrated to each other.

$$dP = \rho g dh \quad (5.1)$$

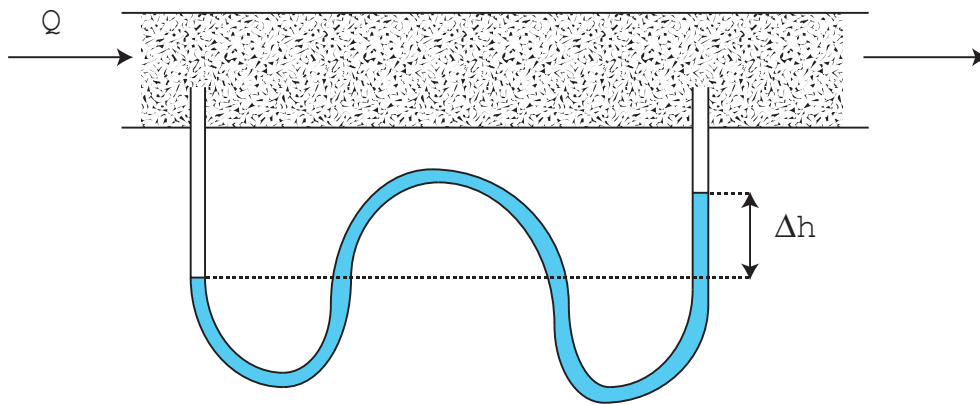


Figure 5.1.: Tube Manometer

### 5.4 Data Logger

A data logger is used to store and monitor the measurements. The measurements shall be analyzed; therefore, it is convenient that the data logger can export the data in a .txt or .xls file. The choice of data logger depends on price, accuracy and number of input channels.

### 5.5 Power Supply

The heating element needs a steady power supply to maintain constant heat flux. The small models that are intended to be built will require relatively small amounts of power; therefore, a power supply that generates up to 50W should be satisfying.

The output power can be calculated by measuring the current  $I$  (Ampere) and voltage  $V$  (Volt). Joule's law:

$$\dot{Q} = I \cdot V \quad (5.2)$$

Where  $\dot{Q}$  is the power,  $I$  is the current and  $V$  is the voltage.

---

---

PART II

---

# Principal Designs

## THERMAL DIFFUSIVITY - CENTERED HEATER

### 6.1 Basis

To make correct measurements, it is important to have control over as many influencing parameters as possible. If the heater is positioned in the center of the sample, the heat loss can be disregarded.

### 6.2 Principal Design

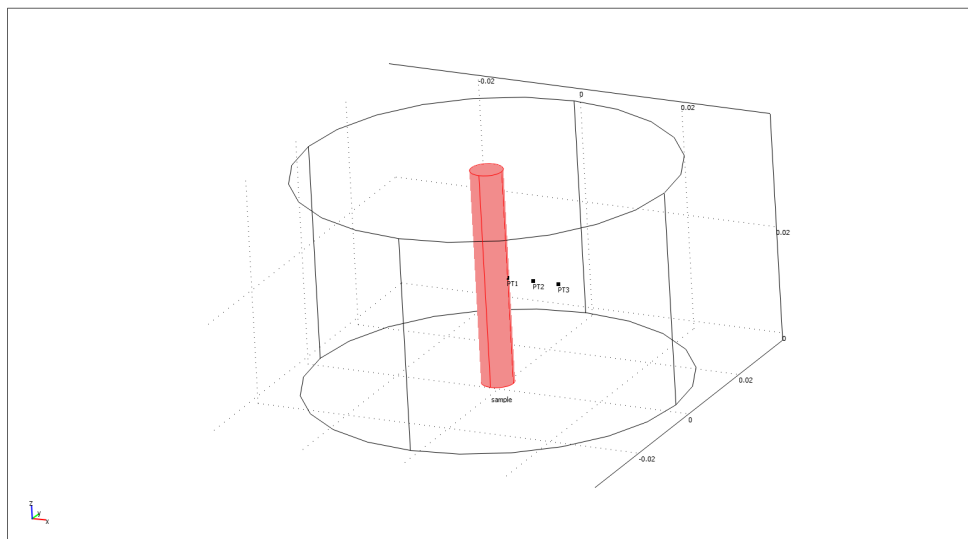


Figure 6.1.: Principal Design

The heater is placed in the center of the sample, and three temperature sensors are installed radially as illustrated. A centered heater makes it possible to put the whole cylinder in a boiling liquid to maintain a constant wall temperature.

### 6.3 Analysis

The test rig is intended to measure thermal diffusivity, but can also measure conductivity.

## 6.3.1. Thermal Diffusivity (TFDA)

The thermal diffusivity can be calculated from temperature measurements at three positions over time. The equation for transient heat conduction from section 4.3.1 is used.

$$\alpha = \frac{T_m^{i+1} - T_m^i}{\frac{8\Delta t}{\pi(r_{m-1}^2 + 2(r_m r_{m+1} - r_{m-1} r_m) - r_{m-1}^2)} \left[ \frac{T_{m-1}^{i+1} - T_m^{i+1}}{\ln(\frac{r_m}{r_{m-1}})} + \frac{T_{m+1}^{i+1} - T_m^{i+1}}{\ln(\frac{r_{m+1}}{r_m})} \right]} \quad (6.1)$$

Note that  $\alpha$  here is solved implicit. The length of the time step is not important in the stability perspective when the equation is solved for thermal diffusivity. The thermal diffusivity is a function of the following variables:

$$\alpha(T_m^{i+1}, T_m^i, T_{m-1}^{i+1}, T_{m+1}^{i+1}, r_{m-1}, r_m, r_{m+1}, \Delta t) \quad (6.2)$$

## Worst Case Error

It is important to consider the consequence of inaccurate measurements; hence, it is appropriate to estimate the worst deviation possible when the tolerances for each variable are defined.

$$\begin{aligned} \Delta \epsilon_{wc} = & \left| \frac{\partial \alpha}{\partial T_m^{i+1}} \right| \Delta T + \left| \frac{\partial \alpha}{\partial T_m^i} \right| \Delta T + \left| \frac{\partial \alpha}{\partial T_{m-1}^{i+1}} \right| \Delta T + \left| \frac{\partial \alpha}{\partial T_{m+1}^{i+1}} \right| \Delta T \\ & + \left| \frac{\partial \alpha}{\partial r_{m-1}} \right| \Delta r + \left| \frac{\partial \alpha}{\partial r_m} \right| \Delta r + \left| \frac{\partial \alpha}{\partial r_{m+1}} \right| \Delta r + \left| \frac{\partial \alpha}{\partial \Delta t} \right| \Delta(\Delta t) \end{aligned} \quad (6.3)$$

## Statistical Error

It is not likely that all errors take place at the same time and in the same direction; therefore, it is better to consider the statistical error when multiple sources of error are present.

$$\begin{aligned} \Delta \epsilon_{st} = & \left[ \left( \frac{\partial \alpha}{\partial T_m^{i+1}} \right)^2 (\Delta T)^2 + \left( \frac{\partial \alpha}{\partial T_m^i} \right)^2 (\Delta T)^2 + \left( \frac{\partial \alpha}{\partial T_{m-1}^{i+1}} \right)^2 (\Delta T)^2 + \left( \frac{\partial \alpha}{\partial T_{m+1}^{i+1}} \right)^2 (\Delta T)^2 \right. \\ & \left. + \left( \frac{\partial \alpha}{\partial r_{m-1}} \right)^2 (\Delta r)^2 + \left( \frac{\partial \alpha}{\partial r_m} \right)^2 (\Delta r)^2 + \left( \frac{\partial \alpha}{\partial r_{m+1}} \right)^2 (\Delta r)^2 + \left( \frac{\partial \alpha}{\partial \Delta t} \right)^2 (\Delta(\Delta t))^2 \right]^{\frac{1}{2}} \end{aligned} \quad (6.4)$$

To illustrate the worst possible and statistical error, a case has been defined where the temperature values are calculated with equation 4.8. The thermal diffusivity was set to  $\alpha = 4 \cdot 10^{-7}$  and time step to  $\Delta t = 10s$ .

$i$	$T_{m-1}$	$T_m$	$T_{m+1}$
1	185.4695	127.0983	95.5738
2	186.0035	127.6746	95.9055
	$r_{m-1}$	$r_m$	$r_{m+1}$
	0.010	0.015	0.020

Table 6.1.: Calculated Temperature Values [K] and Radial Position of Nodes [m]

The nominal value has been calculated with equation 6.1, and the differential expressions have been solved with MAPLE. It is mainly the order of magnitude between the nominal value and error that is interesting.

$$\alpha = \alpha_{nominal} \pm \Delta \epsilon \quad (6.5)$$



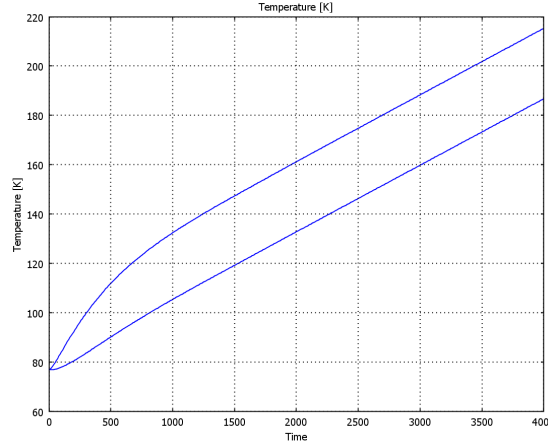
$\Delta T$	$\Delta r$	$\Delta(\Delta t)$	$\alpha_{nominal}$	$\Delta\epsilon_{wc}$	$\frac{\Delta\epsilon_{wc}}{\alpha}$	$\Delta\epsilon_{st}$	$\frac{\Delta\epsilon_{st}}{\alpha}$
0.1	0.0	0.0	$4.06 \cdot 10^{-7}$	$1.41 \cdot 10^{-7}$	0.35	$9.49 \cdot 10^{-8}$	0.23
0.0	0.001	0.0	$4.06 \cdot 10^{-7}$	$1.26 \cdot 10^{-6}$	3.10	$7.91 \cdot 10^{-7}$	1.95
0.0	0.0	0.1	$4.06 \cdot 10^{-7}$	$4.06 \cdot 10^{-9}$	0.01	$4.06 \cdot 10^{-9}$	0.01
0.1	0.001	0.1	$4.06 \cdot 10^{-7}$	$1.41 \cdot 10^{-6}$	3.47	$7.97 \cdot 10^{-7}$	1.96

Table 6.2.: Nominal Values and Errors

Small deviations in the measurements will affect the result; however, it is the placement of the temperature sensors that really is critical. The influence of errors caused by temperature can be reduced with bigger time steps. This is because the temperature difference between the time steps ( $T_m^{i+1} - T_m^i$ ) will increase and be less affected by  $\Delta T$ .

### 6.3.2. Thermal Diffusivity (From Conductivity Equation)

Another approach is to use the solution from the conductivity equation as shown in section 4.3.2. This method is interesting due to its simplicity, see equation 4.13. It is obvious that the less influencing parameters, the better are the chances to achieve proper results. A simulation has been done in COMSOL to review the method.

Figure 6.2.: Temperature development at  $r = 7mm$  and  $r = 15mm$  with insulated outer walls,  $\alpha = 4 \cdot 10^{-7} \frac{m^2}{s}$ 

This method does only work for steady state conditions, figure 6.2 illustrates the transient period that will occur in the beginning. The length of the transient period depends on the thermal properties of the material and the distance between the temperature sensors. Unfortunately, it turns out that equation 4.13 delivers wrong results after having compared it with simulations.

### 6.3.3. Thermal Conductivity

The thermal conductivity can be calculated when the test rig has reached steady state.

$$k = -\frac{\dot{Q}}{2\pi h} \cdot \frac{\ln\left(\frac{r_2}{r_1}\right)}{T_2 - T_1} \quad (6.6)$$

#### Worst Case Error

The worst possible error is investigated in the same way as for the thermal diffusivity:

$$k(\dot{Q}, r_2, r_1, T_2, T_1, h) \quad (6.7)$$

$$\Delta\epsilon_{wc} = \left| \frac{\partial k}{\partial \dot{Q}} \right| \Delta\dot{Q} + \left| \frac{\partial k}{\partial r_2} \right| \Delta r + \left| \frac{\partial k}{\partial r_1} \right| \Delta r + \left| \frac{\partial k}{\partial T_2} \right| \Delta T + \left| \frac{\partial k}{\partial T_1} \right| \Delta T + \left| \frac{\partial k}{\partial h} \right| \Delta h \quad (6.8)$$

*Statistical Error*

$$\Delta\epsilon_{st} = \left[ \left( \frac{\partial k}{\partial \dot{Q}} \right)^2 (\Delta\dot{Q})^2 + \left( \frac{\partial k}{\partial r_2} \right)^2 (\Delta r)^2 + \left( \frac{\partial k}{\partial r_1} \right)^2 (\Delta r)^2 + \left( \frac{\partial k}{\partial T_2} \right)^2 (\Delta T)^2 + \left( \frac{\partial k}{\partial T_1} \right)^2 (\Delta T)^2 + \left( \frac{\partial k}{\partial h} \right)^2 (\Delta h)^2 \right]^{\frac{1}{2}} \quad (6.9)$$

Figure 6.3 shows the steady state profile simulated in COMSOL for a material with conductivity  $k = 0.1 \frac{W}{mK}$ . The diameter of the heater in the middle was  $d = 7mm$  and  $\dot{Q} = 0.77W$ . It has been assumed that all heat is transported radially, and that the wall temperature is constant ( $T = 77K$ ). The test rig reached steady state after approximately one hour.

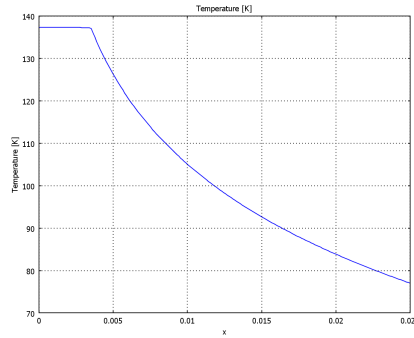


Figure 6.3.: Temperature Profile, Steady State

The following calculations are based on a temperature sensor on the heater ( $T = 138K$ ) and a known wall temperature.

$\Delta T$	$\Delta \dot{Q}$	$\Delta r$	$\Delta h$	$k_{nominal}$	$\Delta\epsilon_{wc}$	$\frac{\Delta\epsilon_{wc}}{k}$	$\Delta\epsilon_{st}$	$\frac{\Delta\epsilon_{st}}{\alpha}$
0.1	0.0	0.0	0.0	0.099	$3.24 \cdot 10^{-4}$	0.00	$3.24 \cdot 10^{-4}$	0.00
0.0	0.1	0.0	0.0	0.099	0.013	0.13	0.013	0.13
0.0	0.0	0.001	0.0	0.099	0.015	0.15	0.015	0.15
0.0	0.0	0.0	0.001	0.099	0.003	0.03	0.003	0.03
0.1	0.1	0.001	0.001	0.099	0.032	0.32	0.020	0.20

Table 6.3.: Nominal Values and Errors

With the assumed inaccuracies, it is possible to get a deviation maximum 30 % from the real value. However, the error will most likely be smaller.

#### 6.4 Cost Estimate

In addition to the steel needed to make the cylinder, the major components of the rig are 1 heating rod, 3 thermocouples, 1 power supply and 1 data logger. A rough cost estimate of relevant components has been made in table 6.4.

## 6.5. CONCLUSION

Component	Manufacturer	Model	Price	
Heating Rod	OMEGA	1/4" Diameter CIR Series	400 NOK	[21]
Thermocouple	Max Sievert A/S	0.25mm Type T	3 · 400 NOK	[15]
Power Supply	Mascot	MA-0719 45W	2000 NOK	[14]
Data Logger	National Instruments	NI9211	2000 NOK	[18]
Data Logger	National Instruments	NI USB-9162	1500 NOK	[17]
<b>Total</b>			<b>7100 NOK</b>	

Table 6.4.: Cost Estimate - Centered Heater

### 6.5 Conclusion

The error analysis points out that accurate positioning of the thermometers are very important. In fact, the positioning for the TFDA method need to be so accurate that it appears to be hard to implement in practice. The TFDA method is easier to use in one dimension since the control volumes are constant for each node.

The thermal diffusivity can also be obtained from the conduction equation. The method will not be pursued further after it turned out to not correspond with the simulation results.

The principal design of this rig is in favor for the conductivity measurement method since the heat loss can be disregarded. However, it is time consuming for the temperature profile to reach steady state. A way to reduce this problem is to decrease the radius of the sample. Another advantage of the design is the simplicity to maintain a constant wall temperature.

To sum it up, a cylindrical test rig with centered heater is most beneficial for steady state conductivity measurements. The method requires only two thermometers and a constant heat rate.

## THERMAL DIFFUSIVITY - HEATER BELOW

### 7.1 Basis

After having evaluated a test rig with centered heater it was experienced that the sensitivity of the sensor positioning was very critical. By placing the heater below the sample, heat will be transferred one dimensionally through the sample. This will result in a simplified expression for the transient finite difference approach.

### 7.2 Principal Design

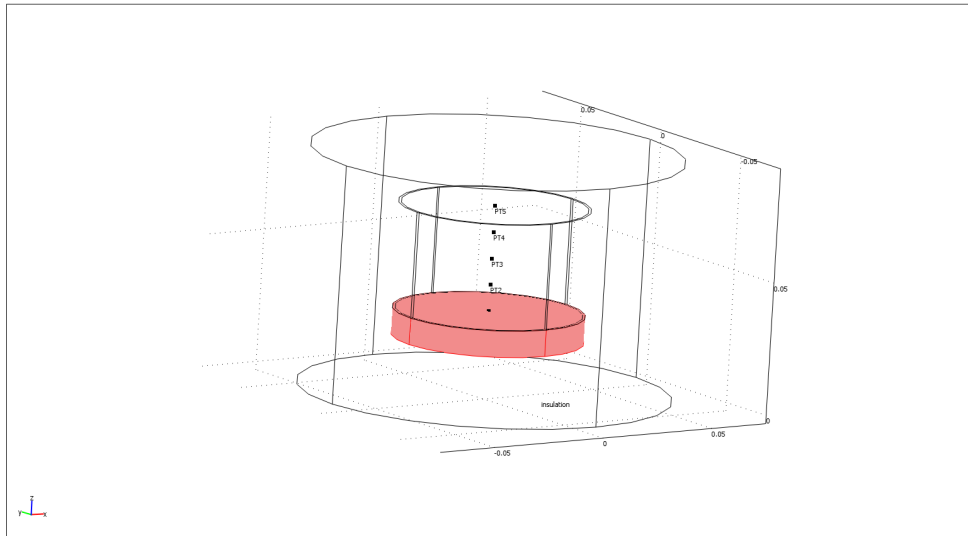


Figure 7.1.: Principal Design - Heater Below

The heater is placed underneath a slender cylinder which contains the sample. A bigger cylinder of insulation encloses the sample and heater. Temperature sensors are placed in one dimension with equal spacing as illustrated in figure 7.1.

### 7.3 Analysis

#### 7.3.1. Thermal Diffusivity (TFDA)

The transient finite difference method was deviated in section 4.3.1:

$$\alpha = \frac{\Delta x^2}{\Delta t} \frac{T_m^{i+1} - T_m^i}{T_{m-1}^i - 2T_m^i + T_{m+1}^i} \quad (7.1)$$

The equation can be solved implicit and explicit.

The expression for thermal diffusivity is evaluated:

$$\alpha(\Delta x, \Delta t, T_m^{i+1}, T_m^i, T_{m-1}^i, T_{m+1}^i) \quad (7.2)$$

#### Worst Case Error

$$\begin{aligned} \Delta \epsilon_{wc} = & \left| \frac{\partial \alpha}{\partial \Delta x} \right| \Delta(\Delta x) + \left| \frac{\partial \alpha}{\partial \Delta t} \right| \Delta(\Delta t) + \left| \frac{\partial \alpha}{\partial T_m^{i+1}} \right| \Delta T \\ & + \left| \frac{\partial \alpha}{\partial T_m^i} \right| \Delta T + \left| \frac{\partial \alpha}{\partial T_{m-1}^i} \right| \Delta T + \left| \frac{\partial \alpha}{\partial T_{m+1}^i} \right| \Delta T \end{aligned} \quad (7.3)$$

#### Statistical Error

$$\begin{aligned} \Delta \epsilon_{wc} = & \left[ \left( \frac{\partial \alpha}{\partial \Delta x} \right)^2 (\Delta(\Delta x))^2 + \left( \frac{\partial \alpha}{\partial \Delta t} \right)^2 (\Delta(\Delta t))^2 + \left( \frac{\partial \alpha}{\partial T_m^{i+1}} \right)^2 (\Delta T)^2 \right. \\ & \left. + \left( \frac{\partial \alpha}{\partial T_m^i} \right)^2 (\Delta T)^2 + \left( \frac{\partial \alpha}{\partial T_{m-1}^i} \right)^2 (\Delta T)^2 + \left( \frac{\partial \alpha}{\partial T_{m+1}^i} \right)^2 (\Delta T)^2 \right]^{\frac{1}{2}} \end{aligned} \quad (7.4)$$

A typical case has been simulated in COMSOL to evaluate the sensitivity. Constant heat flux ( $1000 \frac{W}{m^2}$ ) has been run through a sample with thermal diffusivity of  $\alpha = 4 \cdot 10^{-7}$ , and three temperature sensors with  $\Delta x = 10mm$  spacing have been placed one dimensionally. The temperature at the nodes are shown in table 7.1 with a timestep of  $\Delta t = 30s$ . MAPLE has been used to differentiate the expressions.

$i$	$T_{m-1}$	$T_m$	$T_{m+1}$
1	336.3406	312.3709	305.4642
2	339.3182	314.3791	307.0863

Table 7.1.: Simulated Temperature Values [K] from COMSOL

$\Delta(\Delta x)$	$\Delta(\Delta t)$	$\Delta T$	$\alpha_{nominal}$	$\Delta \epsilon_{wc}$	$\frac{\Delta \epsilon_{wc}}{\alpha}$	$\Delta \epsilon_{st}$	$\frac{\Delta \epsilon_{st}}{\alpha}$
0.001	0.0	0.0	$3.92 \cdot 10^{-7}$	$7.85 \cdot 10^{-8}$	0.20	$7.85 \cdot 10^{-8}$	0.20
0.0	1.0	0.0	$3.92 \cdot 10^{-7}$	$1.31 \cdot 10^{-8}$	0.03	$1.31 \cdot 10^{-8}$	0.03
0.0	0.0	0.1	$3.92 \cdot 10^{-7}$	$4.83 \cdot 10^{-8}$	0.12	$2.83 \cdot 10^{-8}$	0.07
0.001	1.0	0.1	$3.92 \cdot 10^{-7}$	$1.40 \cdot 10^{-7}$	0.36	$8.44 \cdot 10^{-8}$	0.22

Table 7.2.: Nominal Values and Worst Case Error

The sensitivity depends on the positioning of the temperature sensors and their measurement accuracies. Once again, note that the sensitivity will vary in different cases; this is only ment to illustrate the order of magnitude.

The transient finite difference approach seem to work better for one dimensional heat transfer.

### 7.3.2. Thermal Conductivity

The test rig is not suitable for conductivity measurements as it is difficult to measure the heat flux.

### 7.4 Cost Estimate

The major components are the same as for the test rig with centered heater except for the heating rod.

Component	Manufacturer	Model	Price	
Heating Element	Friedr. Freek GmbH	Micanite 65mm Diameter	1000 NOK	[12]
Thermocouple	Max Sievert A/S	0.25mm Type T	3 · 400 NOK	[15]
Power Supply	Mascot	MA-0719 45W	2000 NOK	[14]
Data Logger	National Instruments	NI9211	2000 NOK	[18]
Data Logger	National Instruments	NI USB-9162	1500 NOK	[17]
<b>Total</b>			<b>7700 NOK</b>	

Table 7.3.: Cost Estimate - Heater Below

### 7.5 Conclusion

One dimensional heat flux results in equal control volumes between each temperature sensor; hence, a simplification of the TFDA expression. The thermal diffusivity can be calculated without knowing the actual heat flux which is important since the heater is placed below the sample. The error analysis points out that accurate positioning is important, but not impossible to achieve. This design is not in favor for steady state conductivity measurements.

The principal design will be developed further in chapter 10.

## PERMEABILITY

### 8.1 Basis

It was decided to build a rig for permeability since it not seems to exist any suitable rigs for these measurements at NTNU. The permeability can be measured by sending a flow through a sample and measure the difference in pressure between inlet and outlet.

### 8.2 Principal Design

A vertical pipe is filled with the specimen, and the pressure is measured in the top and bottom of the pipe. The pipe is rotated vertically to obtain an equal distribution of the material in the radial direction.

### 8.3 Analysis

Darcy's law was used to obtain an expression for the permeability in section 4.4.

$$\kappa = \frac{4Q}{\pi D^2} \cdot \frac{\mu}{\frac{P_2 - P_1}{L} - \rho g} \quad (8.1)$$

The pressure drop through the pipe is affected by the permeability of the specimen, the wall friction, and the gravity. Darcy's law does not consider the wall friction; therefore, it is important that the wall friction is small.

$$dP_{\text{permeability}} \gg dP_{\text{wall friction}} \quad (8.2)$$

This analysis assume the wall friction to be neglectable; nevertheless, this assumption needs further investigation.

The permeability measurement requires steady state, it is therefore necessary with a steady flow through the specimen which can be obtained with a pump or compressed air from the laboratory. The pressure drop decrease linearly as illustrated in figure 8.2; hence, the length of the pipe determines the pressure drop. The size of the diameter is insignificant since the wall friction is neglected.

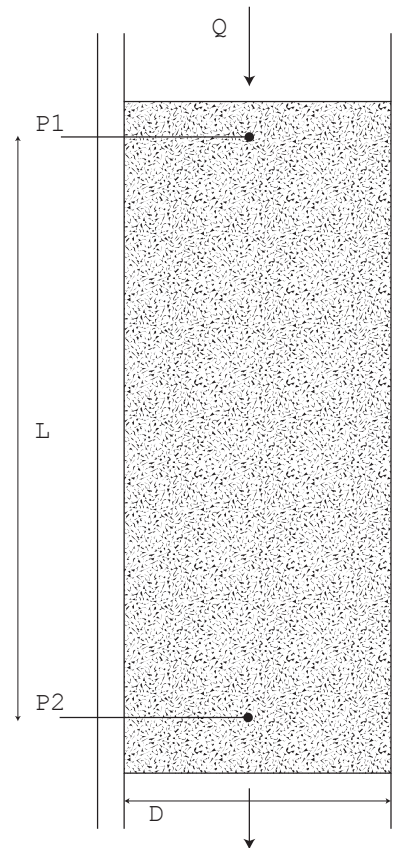


Figure 8.1.: Principal Design

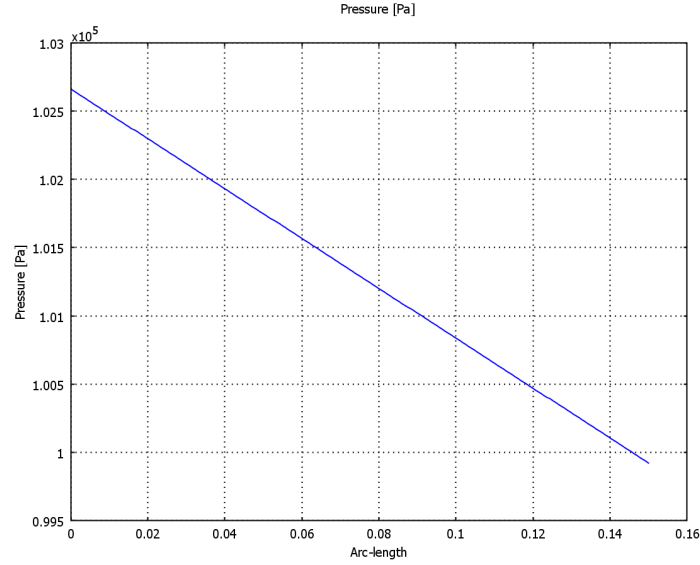


Figure 8.2.: Pressure Drop in the Pipe

The test rig will have relatively small dimensions due to the limited supply of the specimen; this causes a low pressure drop over the pipe which increase the importance of accurate pressure measurements. An error analysis has been done to investigate the error range. The error analysis has been done on a horizontal pipe:

$$\kappa = \frac{u\mu L}{P_2 - P_1} \quad (8.3)$$

$$\kappa = \kappa(u, \mu, L, P_2, P_1) \quad (8.4)$$

*Worst Case Error*

$$\Delta\epsilon_{wc} = \left| \frac{\partial \kappa}{\partial u} \right| \cdot \Delta u + \left| \frac{\partial \kappa}{\partial \mu} \right| \cdot \Delta \mu + \left| \frac{\partial \kappa}{\partial L} \right| \cdot \Delta L + \left| \frac{\partial \kappa}{\partial P_2} \right| \cdot \Delta P + \left| \frac{\partial \kappa}{\partial P_1} \right| \cdot \Delta P \quad (8.5)$$

*Statistical Error*

$$\Delta\epsilon_{st} = \left[ \left( \frac{\partial \kappa}{\partial u} \right)^2 (\Delta u)^2 + \left( \frac{\partial \kappa}{\partial \mu} \right)^2 (\Delta \mu)^2 + \left( \frac{\partial \kappa}{\partial L} \right)^2 (\Delta L)^2 + \left( \frac{\partial \kappa}{\partial P_2} \right)^2 (\Delta P)^2 + \left( \frac{\partial \kappa}{\partial P_1} \right)^2 (\Delta P)^2 \right]^{\frac{1}{2}} \quad (8.6)$$

A simulation has been done in COMSOL for a 150mm long pipe with air flowing through at  $u = 1 \frac{m}{s}$ , the pressure drop is plotted in figure 8.2. The permeability was set to  $\kappa = 10^{-9} m^2$ . The differential expressions have been solved with MAPLE.

The pressure sensors should have an accuracy within 100Pa which is fully obtainable.

#### 8.4 Cost Estimate

The main components of the permeability rig are: 1 inclined tube manometer, 1 precision valve, 1 flow meter, and 1 inlet filter. Compressed air from the laboratory will be used as the working fluid. The cost estimate is a rough calculation based on prices found on the internet.



## 8.5. CONCLUSION

$\Delta u$	$\Delta \mu$	$\Delta L$	$\Delta P$	$\kappa_{nominal}$	$\Delta \epsilon_{wc}$	$\frac{\Delta \epsilon_{wc}}{\kappa}$	$\Delta \epsilon_{st}$	$\frac{\Delta \epsilon_{st}}{\kappa}$
0.1	0.0	0.0	0.0	$10^{-9}$	$10^{-10}$	0.10	$10^{-10}$	0.10
0.0	$10^{-6}$	0.0	0.0	$10^{-9}$	$5.48 \cdot 10^{-11}$	0.05	$5.48 \cdot 10^{-11}$	0.05
0.0	0.0	0.01	0.0	$10^{-9}$	$6.67 \cdot 10^{-11}$	0.07	$6.67 \cdot 10^{-11}$	0.07
0.0	0.0	0.00	100	$10^{-9}$	$7.31 \cdot 10^{-11}$	0.07	$5.17 \cdot 10^{-11}$	0.05
0.1	$10^{-6}$	0.01	100	$10^{-9}$	$2.95 \cdot 10^{-10}$	0.29	$1.42 \cdot 10^{-10}$	0.14

Table 8.1.: Nominal Values and Errors

Component	Manufacturer	Model	Price	
Inclined Tube Manometer	Systronik	P2601	2700 NOK	[11]
Precision Valve	Nordgren	VP50	4700 NOK	[20]
Flow Meter	Key Instruments	FL MTR AIR 14-140 LPM	1400 NOK	[13]
Filter	Nordgren	BL64	2000 NOK	[19]
<b>Total</b>			<b>10800 NOK</b>	

Table 8.2.: Cost Estimate - Permeability Rig

### 8.5 Conclusion

Measurement of permeability should be fully achievable in the perspective of possible errors due to measurement inaccuracies. The geometry of the rig needs further analysis to optimize the ratio of diameter compared to length. An optimal ratio should justify the assumption of neglectable wall friction.

---

---

## PART III

---

# Completion

## TEST RIG FOR THERMAL CONDUCTIVITY

### 9.1 Basis

It turns out that there has been built a test rig for measurement of conductivity earlier, the rig is still in the laboratory of this department. In the starting point it was not intended to build this rig, but as it already exists, it seems convenient to give it a try.

The rig was built by E. Mikkelsen and M. Lamvik and was used for steady state measurements of conductivity.

### 9.2 Experimental Method [5] and Equipment

A heating rod with 4mm outer diameter and 350mm length is placed in center of the cylinder. An electric heating element with length 200mm is placed inside the heating rod. Two thermocouples type K are placed at the midpoint of the heating element at two different radii. The outer diameter of the thermocouples are 0.5mm. Water tubes are wrapped around the sample cylinder to maintain a constant wall temperature. The temperature on the inlet and outlet of the water are measured to ensure that it is constant. If the temperature difference is big, the flowrate will be increased. A complete process and instrumentation diagram is attached in appendix A.2.

The rig use the principle explained in section 6.3.3. This kind of measurement can be rather time-consuming since we have to wait for a steady state temperature profile (see figure 6.3).

### 9.3 Test and Adjustments

The first test took place 23 november and confirmed that conductivity measurements are time-consuming processes. When the test was finished after approximately two hours, the temperature profile had not reached steady state. The specimen of sand that was used have a conductivity within  $0.1 - 0.25 \frac{W}{mK}$ , which is in the expected range of MOF. It was also experienced that the wall temperature differed considerably from the cooling water temperature due to a air gap between the sample cylinder and water tubes. The temperature on the water inlet and outlet where

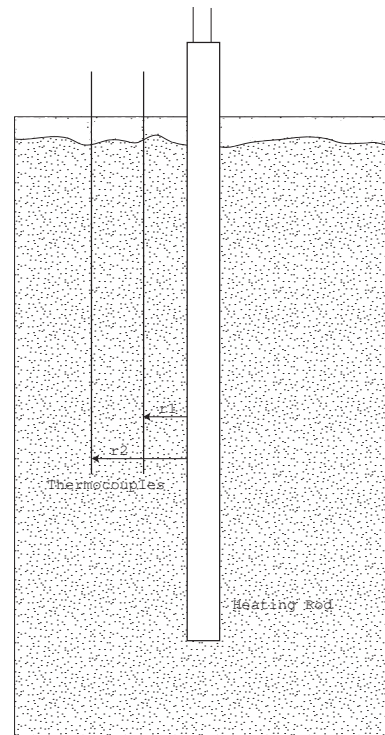


Figure 9.1.: Measurement Setup

measured to be equal during the whole test. Therefore, it was decided to move the thermocouple from the water outlet to the heating rod. Three temperature measurements in radial direction makes the TFDA method possible. It was also decided to make a new cylinder with a smaller diameter with the water tube directly attached. The measurement results are attached in appendix B.



Figure 9.2.: Test Rig - New Cylinder Filled with Sand

### 9.4 Evaluation of Data

Fourier's law of heat conduction (equation 6.6) is used to calculate the conductivity. The accuracy can be estimated to be within  $\pm 20\%$  according to Lamvik [5]. The positioning of the thermocouples are emphasized to be the main source of error. It is assumed that the positioning is within  $\pm 0.5\text{mm}$  of the desired radius. The evaluation of data is straightforward when the temperature profile has reached steady state; it is only necessary to implement the measured temperatures and power output to equation 6.6.

Another approach is to log the transient progress, and use the TFDA method. It turns out that fluctuations in the temperature measurements makes it important to choose a certain step length when calculating the thermal diffusivity. Temperature fluctuations under small time steps gives negative temperature gradients (at node  $m$ ) which leads to negative thermal diffusivity. The problem is shown in figure B.1.

#### 9.4.1. Smoothing of Temperature Measurements

The fluctuations can also be removed by smoothing:

$$\bar{T} = \frac{1}{2n+1} \sum_{i=-n}^n T_i \quad (9.1)$$

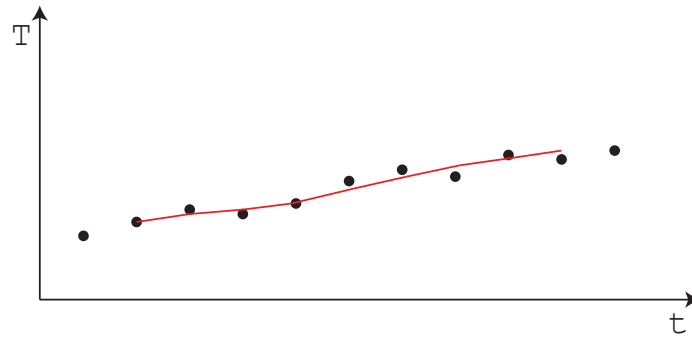


Figure 9.3.: Smoothing of Fluctuations

The purpose of smoothing is to keep the temperature gradient  $\frac{dT}{dt}$  constant positive or negative.

### 9.5 Measurement Results

There have been carried out two TFDA measurements and one steady state measurement, the results are attached in appendix B. The specimen material has been sand for all of the experiments. For the TFDA measurements it is obvious that the inaccuracies are growing as the rig reaches steady state. It is not known why the average thermal diffusivity differ with approximately  $0.7 \frac{m^2}{s}$  in appendix B.1 and B.3. A possible source of error is the positioning of the thermocouples as the two measurements were performed with different cylinders.

The conductivity measurement in appendix B.2 were calculated in three ways since three thermocouples were used. The results are quite similar with an average of  $k = 0.46 \frac{W}{mK}$  which was higher than expected. Unfortunately, the exact properties of the specimen are not known.

More measurements are necessary to verify the current results; nonetheless, it can be said that the rig must be improved to deliver more accurate results. It is also clear that the thermal conductivity measurements are more accurate than the thermal diffusivity measurements.

## TEST RIG FOR THERMAL DIFFUSIVITY

### 10.1 Basis

It was decided to develop the test rig for thermal diffusivity with one dimensional heat flux further after having done the error analysis.

### 10.2 Choice of Materials and Dimensions

Due to limited amounts of the test material it is convenient to make the test rig as small as possible. On the other hand, it is difficult to obtain one-dimensional heat flux in the center if the diameter is too small. Another important factor is the thermal diffusivity of the materials that will enclose the test material; they need to be lower to ensure that the heat will transfer through the specimen.

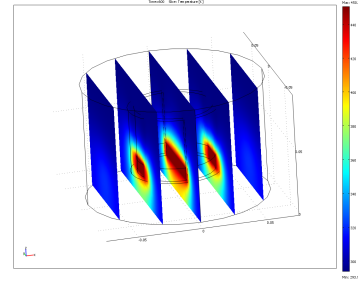


Figure 10.1.: Temperature Distribution

#### 10.2.1. Procedure

A procedure was made to save some time under the selection of the dimensions and material properties of the test rig. The model was sketched in COMSOL, and the position of the temperature nodes was implemented. COMSOL was used for simulations, and the temperature data was exported to MATLAB where the TFDA method was applied. The choice of materials and dimensions was approved when the TFDA method was able to give approximately the same thermal diffusivity as the one used in the simulations.

#### 10.2.2. Materials

There are three main parts of the test rig that concerns the choice of materials: the heating element, the cylinder, and the insulation. In order to ensure one-dimensional heat flux, it is important that the cylinder and insulation have lower thermal diffusivity than the specimen. The diffusivity of the specimen is obviously not known; therefore, it has been assumed to be in the region of  $\alpha = 4 \cdot 10^{-7} \frac{m^2}{s}$ .

$$\alpha = \frac{k}{\rho C_p} \approx \frac{0.1 \frac{W}{mK}}{500 \frac{kg}{m^3} \cdot 500 \frac{J}{kgK}} = 4 \cdot 10^{-7} \frac{m^2}{s} \quad (10.1)$$

The ability of the heating element to transfer heat influences the response time of the measurements; therefore, a material with high thermal diffusivity is preferable. Copper has a thermal

diffusivity in the order of  $\alpha = 10^{-4} \frac{m^2}{s}$  [10] and was selected in front of aluminium which has a slightly lower diffusivity ( $\alpha = 9 \cdot 10^{-5} \frac{m^2}{s}$  [8]). The heating element has been simulated as a copper element with heat flux underneath. In practice, this could be done by attaching hot-wire underneath the copper element.

Both plexiglass (PMMA) and teflon (PFTE) were considered to be suitable materials for the cylinder walls with approximately the same thermal diffusivity of  $\alpha = 10^{-7} \frac{m^2}{s}$  [24] [22]. Teflon is more resistant to higher temperatures than plexiglass; on the other hand, it is harder to fabricate. It was decided to use plexiglass.

The whole cylinder will be enclosed with insulation to lower heat dissipation in other directions than through the specimen. Styrofoam HD300 [25] will be used due to its low conductivity and simplicity to shape.

### 10.2.3. Dimensioning

The procedure was applied to find the minimal diameter with the selected materials. The spacing between the temperature nodes were held constant at  $\Delta x = 10mm$ . It turned out to be more difficult than expected to obtain one-dimensional heat flux; mainly because of the assumed low conductivity of the specimen. The simulation results and thermal diffusivity calculations can be found in appendix C.

It was concluded that the rig should have an inner diameter of  $D_i = 130mm$  to give proper results.

## 10.3 Data Reduction

Data logging of the transient temperature progress gives great amounts of information; as a result, it is necessary to treat the data. First of all, the data must be smoothed as described in section 9.4.1 to remove fluctuations. Secondly, the calculated diffusivity should be presented in tabular form for different temperatures.

$T_{min}$	$\alpha(T_{min})$
$T_{min} + dT$	$\alpha(T_{min} + dT)$
$T_{min} + 2dT$	$\alpha(T_{min} + 2dT)$
$\vdots$	$\vdots$
$\vdots$	$\vdots$
$T_{max}$	$\alpha(T_{max})$

Table 10.1.: Thermal Diffusivity in Tabular Form

### 10.3.1. Linear Interpolation

The thermal diffusivity is a function of temperature,  $\alpha = \alpha(T)$ . It is assumed that a calculated thermal diffusivity is the diffusivity at the current temperature of the node,  $\alpha = \alpha(T_m)$ . The thermal diffusivity can then be tabulated with linear interpolation.

$$\alpha(T) = \frac{\alpha(T_2) - \alpha(T_1)}{T_2 - T_1} \cdot (T - T_1) + \alpha(T_1) \quad (10.2)$$

The data can easily be tabulated by using equation 10.2 when  $T_1 < T < T_2$ , this feature is implemented in the procedure described in section 10.2.1.

## 10.4 Positioning

It has been emphasized that the positioning of the temperature nodes are important. The possible error will be minimized by use of thermocouples with a diameter of 0.25mm. To ensure that they are in the correct position, they will be held in cannula tubes under filling of the specimen.

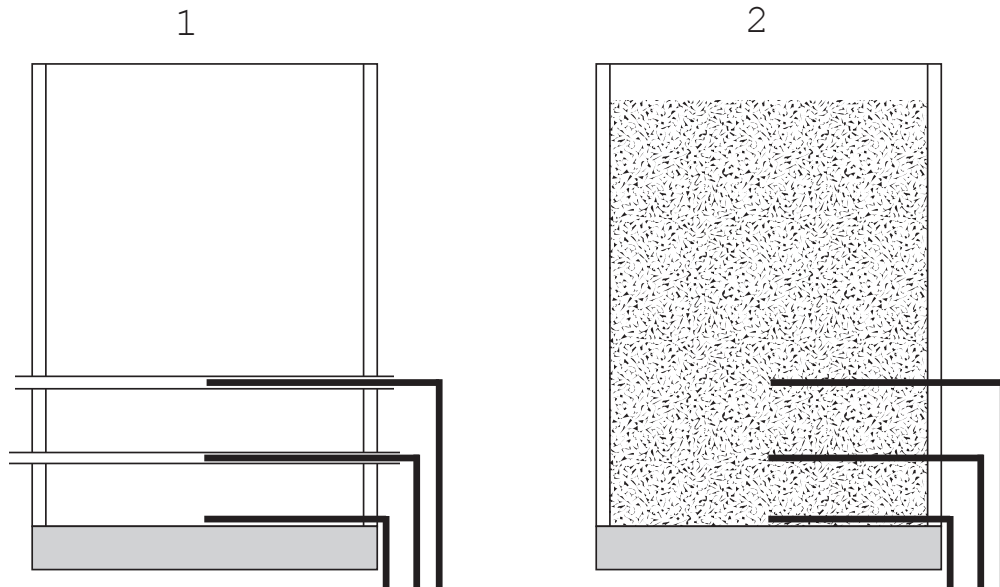


Figure 10.2.: Positioning of Thermocouples

Figure 10.2 illustrates how the thermocouples are held in the correct position under filling of the cylinder (1), the cannula tubes will be removed and the holes sealed after the specimen are in the cylinder (2).

#### **10.5 Completion**

The test rig have not been built due to delays of the ordered thermocouples. Presumably, it will be built in the beginning of next year. The question of the test rigs ability to deliver proper results are however already doubtful. The results from the simulations in appendix C states that it is difficult to obtain a constant value for the thermal diffusivity. Hopefully, practical experience will help to improve the rig.



## CLOSURE

### **11.1** Conclusion

#### *11.1.1. Relevant Measurement techniques*

Definite suggestions have been given for measurements of the thermal properties of the MOF. The specific heat capacity, density and porosity will be measured with existing equipment located at NTNU. For the thermal conductivity and permeability, there have been developed test rigs that presumably will be built next year.

#### *11.1.2. Thermal Diffusivity*

A new measuring technique for thermal diffusivity (TFDA) has been investigated, both radially and in one dimension. The method is applicable for the transient part of a heating process which have a tendency to be long-lasting. The thermal conductivity can be used to calculate the thermal conduction when the specific heat and density are known.

Measurements of the thermal diffusivity with the TFDA method was in the beginning assumed to simplify and shorten the time-length each experiment. In principle, it should be enough to log the temperatures at three points without knowing the actual heat flux. However, simulations for both rigs and measurements on the radial rig have shown that it is difficult to obtain a constant value for the diffusivity. Possible sources of errors have been investigated, and the positioning of the sensors have been found to be the most important factor. The radial rig seems in fact to be too sensitive for any displacements of the sensors. Therefore, it has been concluded that a test rig with centered heater are more suitable for steady state conductivity measurements.

The development of the test rig for one dimensional heat transfer was taken further since the range of errors were noticeable smaller. One-dimensional heat transfer simplifies the expression for the TFDA method as the control volumes are constant for each node. Simulations have shown that a certain diameter is required to obtain one-dimensional heat flux in the center. Even with constant heat flux in the center, it has turned out to be difficult to obtain a constant value for the diffusivity. The rig has not been built due to delivering delays of the ordered components.

The conduction equation has been solved in order to find another expression for the thermal diffusivity. It resulted in a relatively simple equation suitable for measurements. The method is based on a rig with centered heater and insulated outer walls. However, the method was not able to find the thermal diffusivity used in simulations and was therefore dismissed.

To sum it up, it seems to be more difficult than expected to measure the thermal diffusivity properly. None of the simulations or measurements are able to deliver a constant value.

### 11.1.3. Thermal Conduction

Fourier's law of heat conduction has been applied to calculate the thermal conductivity. The method requires that the temperature profile has reached steady state. Depending on the geometry of the rig and specimen, this might be a time-consuming process. The heat flux must be measured to calculate the conductivity; therefore, it is preferable to use a rig with centered heater so heat loss can be disregarded. An error analysis has been performed to identify possible sources of error. Again, accurate positioning seem to be most important, but the magnitude of possible errors are noticeable less than for the TFDA method.

Conductivity measurements have been performed on the existing radial rig. The temperature profile reached steady state relatively fast when a new smaller cylinder with a water tube directly attached was used. The results from the measurements were constant and clear. Consequently, steady state measurements conductivity measurements are considered to be the best measuring method.

### 11.1.4. Permeability

The permeability can be found by measuring the pressure drop for a fluid flowing through the MOF in a pipe. Darcy's law has been evaluated in terms of possible errors, and the results show that the tolerances are fully achievable. The influence of wall friction in the pipe has not been considered.

## **11.2 Further Developments**

The results from this report indicates that steady state measurements in a test rig with centered heater are the best way to obtain the thermal conductivity. A rig with smaller diameter and smaller thermocouples should be built. In addition, a reliable solution for ensurance of correct positioning of the temperature sensors should be developed.

The one dimensional test rig for thermal diffusivity will be built next year. Comparison of real measurements and simulations will hopefully carry along new knowledge which can be used to improve the rig. The TFDA method are at this time not considered to be reliable.

Regarding the permeability rig should the influence of wall friction be further examined. This can be done in practice by measuring the pressure drop over pipes with different diameters and equal length.

---

---

PART IV

---

Appendices

A.1 Thermal Diffusivity - Heater Below

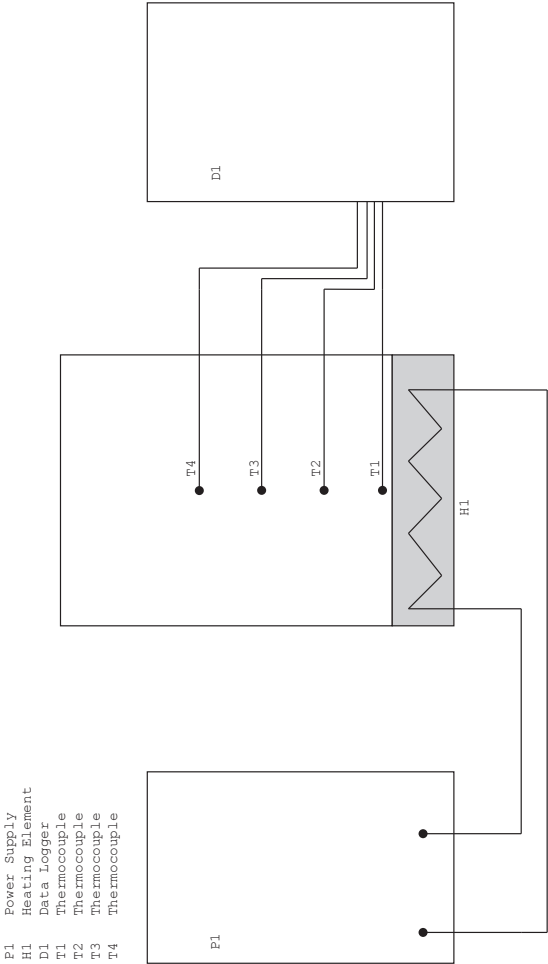


Figure A.1.: P&ID - Heater Below

A.2 Thermal Diffusivity - Centered Heater

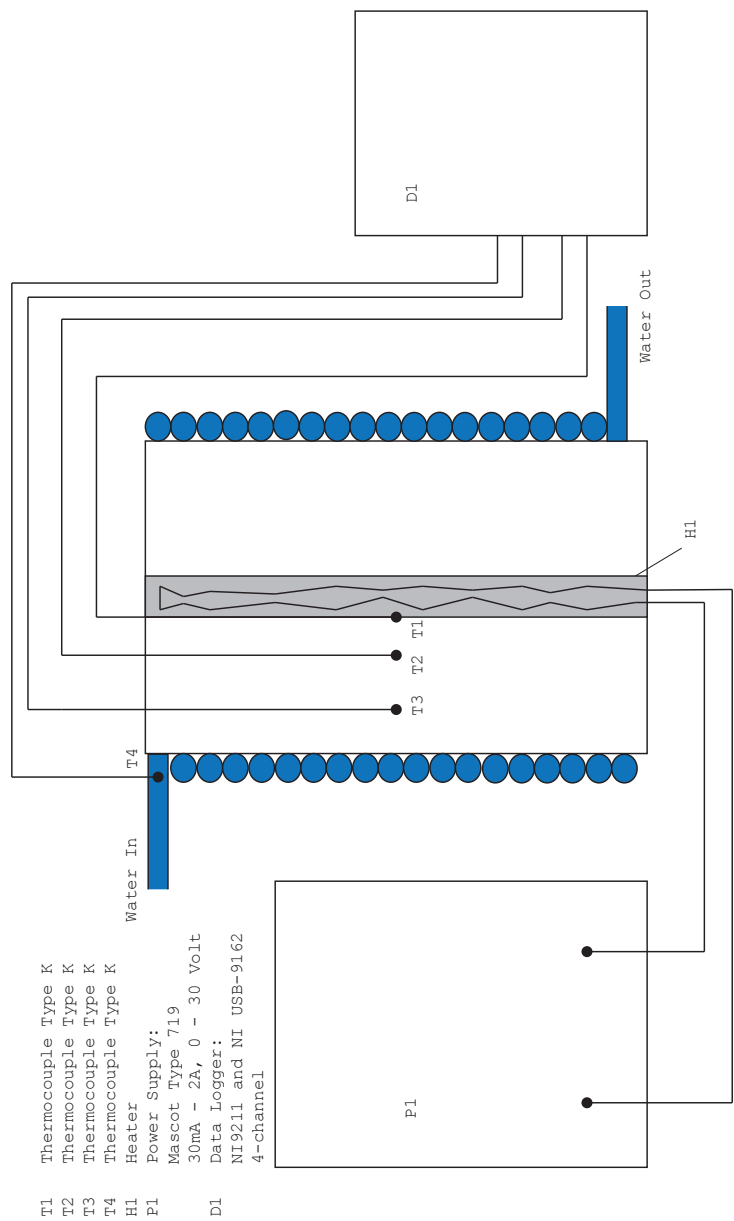


Figure A.2.: P&ID - Centered Heater

## MEASUREMENT RESULTS RADIAL RIG

**B.1** 25 November 2009

Measurement Data		Thermocouple Position	
Date of Measurement	25 November 2009	$r_1$	$2.25 \cdot 10^{-3} m$
Duration	3600s	$r_2$	$15.9 \cdot 10^{-3} m$
$\frac{\dot{Q}}{h}$	$40 \frac{W}{m}$	$r_3$	$24.9 \cdot 10^{-3} m$
$\Delta t$	1s		
Specimen Material	Sand		

Table B.1.: Measurement Setup

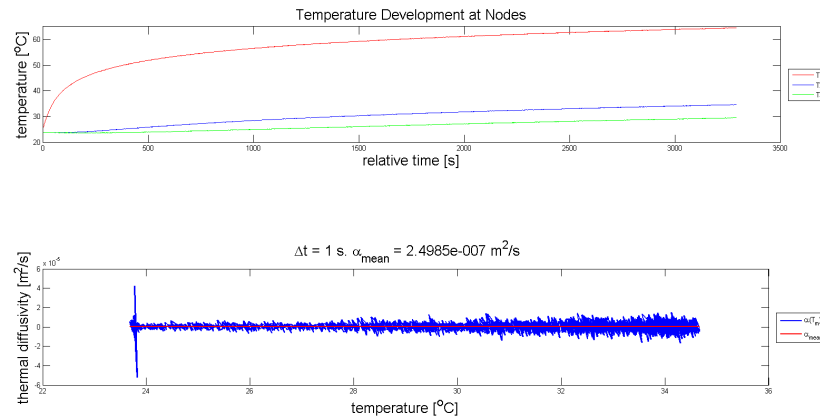


Figure B.1.: Temperature and Thermal Diffusivity Development

*Comments*

Figure B.1 shows signs of disturbance since the change in temperature per time step is smaller than the measurement fluctuations. This is discussed further in section 9.4. The influence of the fluctuations can be reduced by increasing the time step. In addition, the calculation should not be started until the heat has reached the second sensor (approximately 200s on figure B.1). An improved thermal diffusivity calculation is shown in figure B.2.

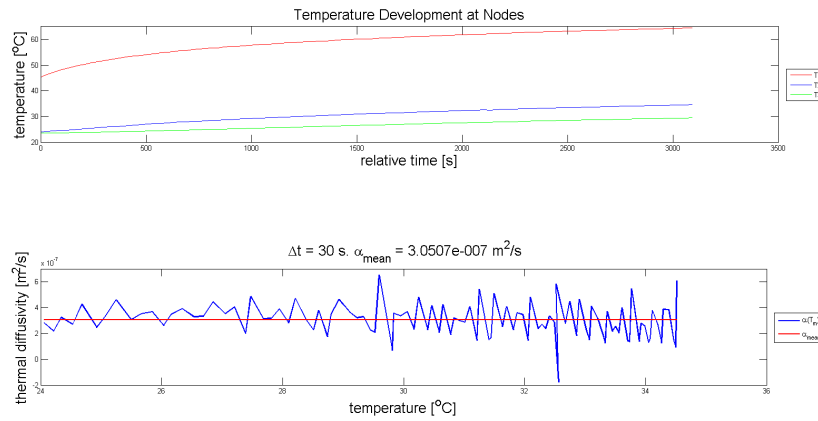


Figure B.2.: Temperature and Thermal Diffusivity Development

### *Sand Properties*

The sand properties has been retrieved from [1, page 853]. It is not known how well they match the actual properties on the sand that was used.

$$\alpha = \frac{k}{\rho C_p} = \frac{0.2 \frac{W}{mK}}{1515 \frac{kg}{m^3} \cdot 800 \frac{J}{kgK}} = 1.65 \cdot 10^{-7} \frac{m^2}{s} \quad (B.1)$$

**B.2** 1 Desember 2009

Measurement Data		Thermocouple Position	
Date of Measurement	1 Desember 2009	$r_1$	$2.25 \cdot 10^{-3}m$
Duration	3600s	$r_2$	$15.9 \cdot 10^{-3}m$
$\frac{\dot{Q}}{h}$	$40 \frac{W}{m}$	$r_3$	$24.9 \cdot 10^{-3}m$
$\Delta t$	1s		
Specimen Material	Sand		

Table B.2.: Measurement Setup

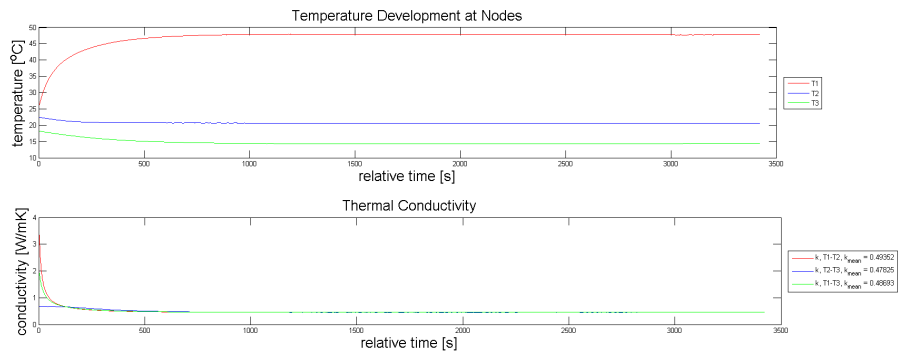


Figure B.3.: Temperature and Conductivity Development

The rig reached steady state after approximately 20 minutes, figure B.4 focuses on the steady state part of the measurement.

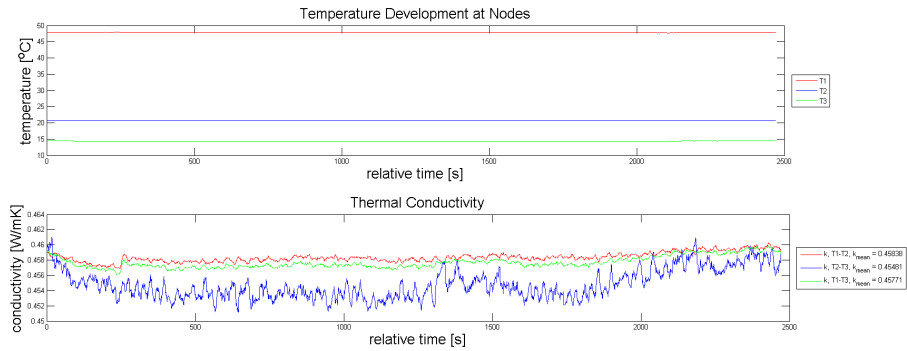


Figure B.4.: Temperature and Conductivity Development

*Comments*

A new cylinder of steel has been made to improve the rapidity of the rig. The water tube is directly attached to the steel to ensure constant wall temperature. This was difficult with the previous cylinder due to the air gap between the cylinder and the water tube.



**B.3** 7 Desember 2009

Measurement Data		Thermocouple Position	
Date of Measurement	7 Desember 2009	$r_1$	$2.25 \cdot 10^{-3} m$
Duration	3600s	$r_2$	$15.9 \cdot 10^{-3} m$
$\frac{\dot{Q}}{h}$	$40 \frac{W}{m}$	$r_3$	$24.9 \cdot 10^{-3} m$
$\Delta t$	1s		
Specimen Material	Sand		

Table B.3.: Measurement Setup

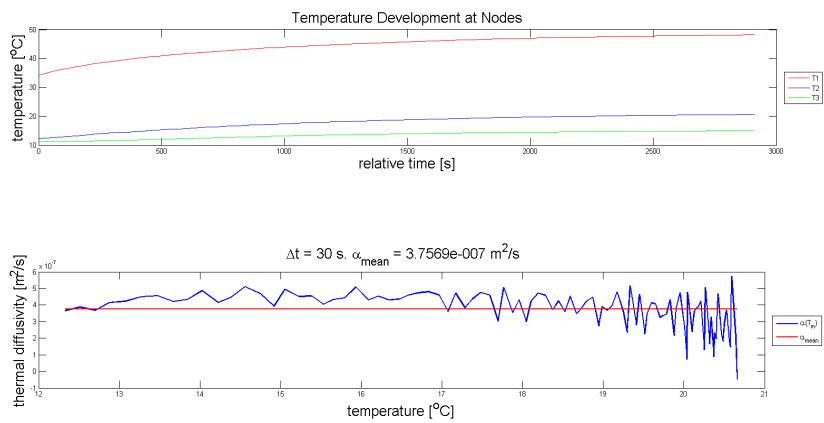


Figure B.5.: Temperature and Thermal Diffusivity Development

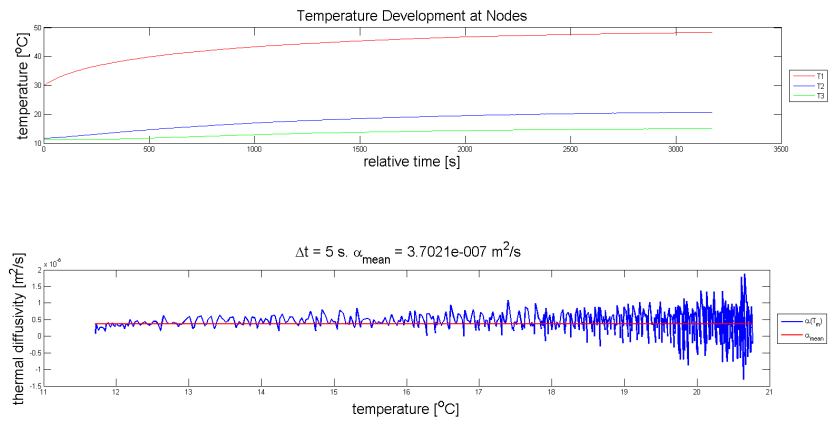


Figure B.6.: Temperature and Thermal Diffusivity Development

*Comments*

The fluctuations are smoothed out with the technique used in section 9.4.1. The inaccuracies increases at the end of the measurement when the transient period is about to end.

## DIMENSIONING OF TEST RIG FOR THERMAL DIFFUSIVITY

### C.1 Basis

The procedure for the dimensioning is described in section 10.2.1. The model consists of the test sample in the center with a copper heating element underneath. A cylinder of plexiglass encloses the specimen, the model is coated by a cylinder of styrofoam.

The goal is to find the smallest possible diameter which results in one dimensional heat flux in the center. The thermal diffusivity of the specimen has been  $\alpha = 4 \cdot 10^{-7} \frac{m^2}{s}$  for all of the simulations.

### C.2 Case 1

#### Input Data for Simulation

Simulation Program	COMSOL Multiphysics 3.4
Boundary Condition	Outer cylinder (Styrofoam) is insulated
Boundary Condition	Upward heat flux discontinuity underneath copper element
Simulation time, $t$	2400s
$\frac{\dot{Q}}{A}$	$2000 \frac{W}{m^2}$
<b>Geometry</b>	
Plexiglass cylinder inner diameter, $D_i$	110mm
Plexiglass cylinder outer diameter, $D_o$	120mm
Spacing temperature nodes, $\Delta x$	10mm

Table C.1.: Simulation Input Data

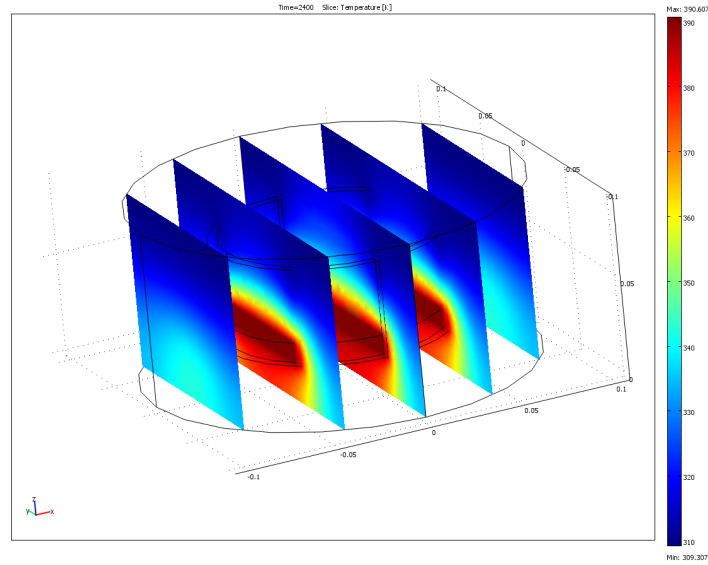


Figure C.1.: Temperature Distribution at  $t = 2400s$ ,  $D_i = 110mm$

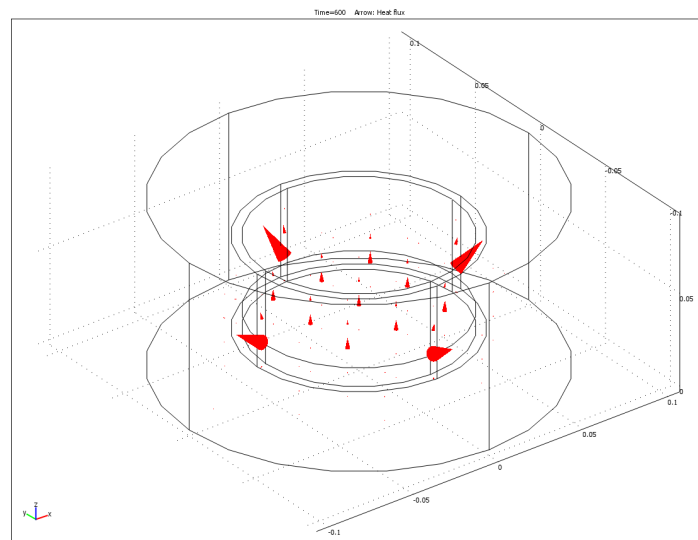


Figure C.2.: Heat Flux at  $t = 600s$ ,  $D_i = 110mm$

The simulated temperature values were exported to MATLAB where the thermal diffusivity was calculated. The thermal diffusivity is plotted as a function of the current temperature at the node, both explicit and implicit. The TFDA method is able to calculate approximately the correct diffusivity in average.

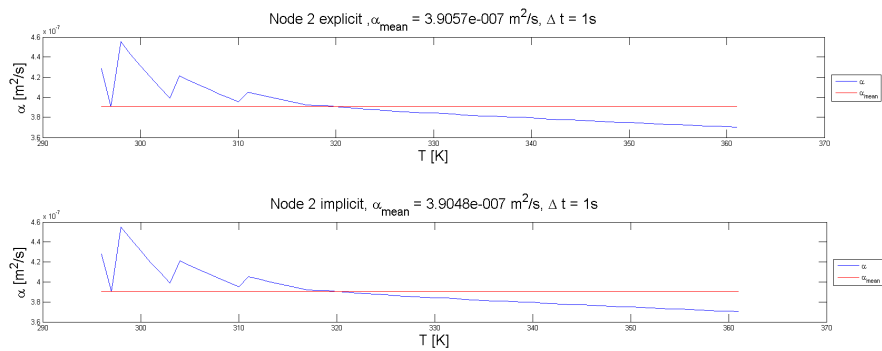


Figure C.3.: Thermal Diffusivity Calculation,  $D_i = 110mm$

C.3 Case 2

Input Data for Simulation	
Simulation Program	COMSOL Multiphysics 3.4
Boundary Condition	Outer cylinder (Styrofoam) is insulated
Boundary Condition	Upward heat flux discontinuity underneath copper element
Simulation time, $t$	2400s
$\frac{\dot{Q}}{\bar{A}}$	$2000 \frac{W}{m^2}$
Geometry	
Plexiglass cylinder inner diameter, $D_i$	60mm
Plexiglass cylinder outer diameter, $D_o$	70mm
Spacing temperature nodes, $\Delta x$	10mm

Table C.2.: Simulation Input Data

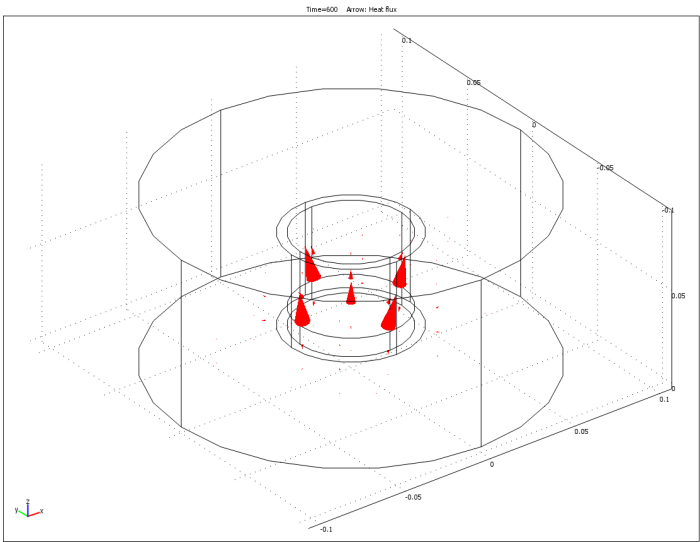


Figure C.4.: Heat Flux at  $t = 600s$ ,  $D_i = 60mm$

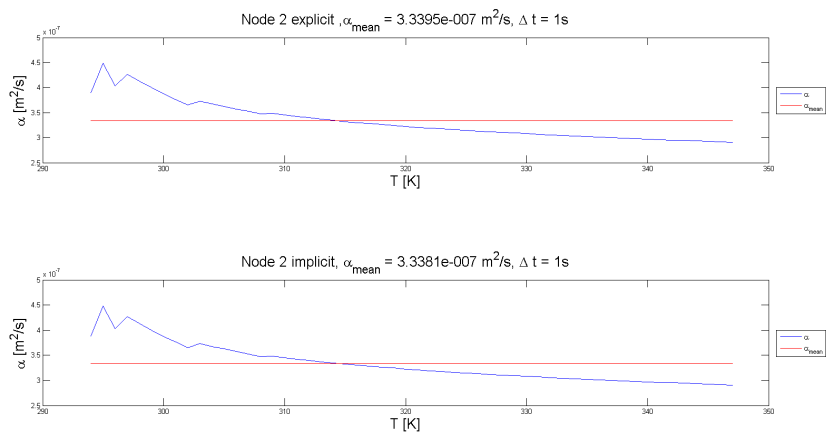


Figure C.5.: Thermal Diffusivity Calculation,  $D_i = 60\text{mm}$

C.4 Case 3

Input Data for Simulation	
Simulation Program	COMSOL Multiphysics 3.4
Boundary Condition	Outer cylinder (Styrofoam) is insulated
Boundary Condition	Upward heat flux discontinuity underneath copper element
Simulation time, $t$	2400s
$\frac{\dot{Q}}{A}$	$2000 \frac{\text{W}}{\text{m}^2}$
Geometry	
Plexiglass cylinder inner diameter, $D_i$	150mm
Plexiglass cylinder outer diameter, $D_o$	160mm
Spacing temperature nodes, $\Delta x$	10mm

Table C.3.: Simulation Input Data

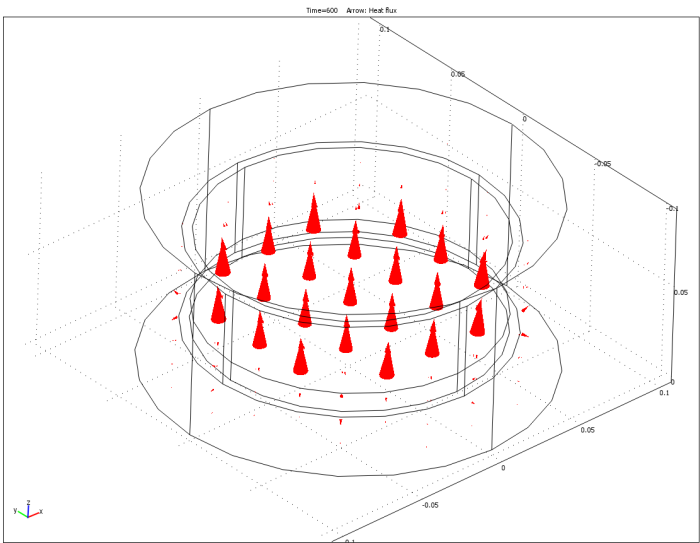
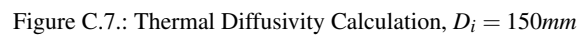


Figure C.6.: Heat Flux at  $t = 600\text{s}$ ,  $D_i = 150\text{mm}$



**C.5**

Simulation Program	COMSOL Multiphysics 3.4
Boundary Condition	Outer cylinder (Styrofoam) is insulated
Boundary Condition	Upward heat flux discontinuity underneath copper element
Simulation time, $t$	2400s
$\frac{\dot{Q}}{A}$	$2000 \frac{W}{m^2}$
<b>Geometry</b>	
Plexiglass cylinder inner diameter, $D_i$	130mm
Plexiglass cylinder outer diameter, $D_o$	140mm
Spacing temperature nodes, $\Delta x$	10mm

Table C.4.: Simulation Input Data

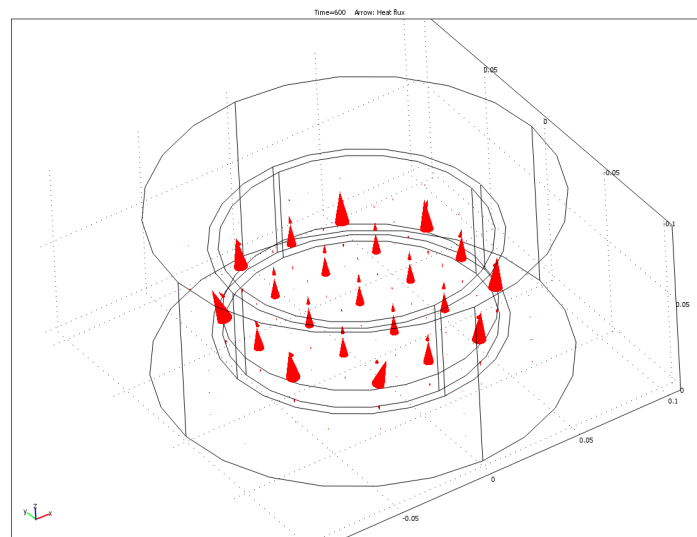


Figure C.8.: Heat Flux at  $t = 600s$ ,  $D_i = 130mm$

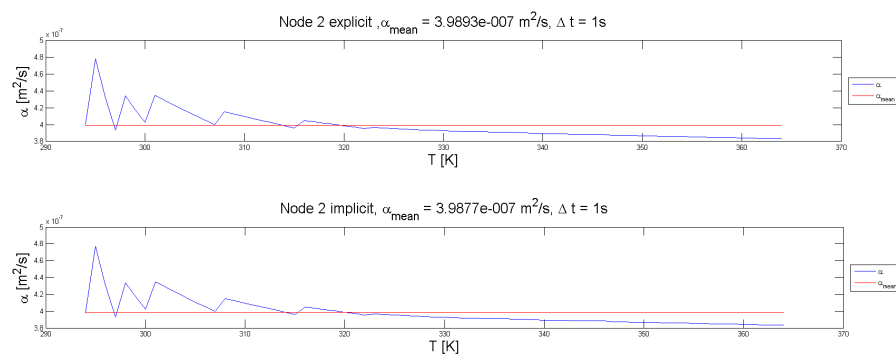


Figure C.9.: Thermal Diffusivity Calculation,  $D_i = 130\text{mm}$

The rig should have an inner diameter  $D_i = 130\text{mm}$  to obtain one dimensional heat flux.

## MEASUREMENT OF DENSITY

### **D.1** Mettler Toledo AT261 [16]

The AT261 is a highly accurate weight with a readability of 0.01mg. It is located at department of energy and process engineering at NTNU.



Figure D.1.: Mettler AT261



## MEASUREMENT OF SPECIFIC HEAT

**E.1** TGA Q500 [26]

The Q500 is a popular research-grade thermogravimetric analyzer. It is based on the same principle as described in section 4.6, and is operated by the department of chemical engineering at NTNU.

The specimen will be put on a small plate and heated; the heat required to raise the temperature a certain step compared to a reference case determines the specific heat capacity.



Figure E.1.: TGA Q500

## MEASUREMENT OF POROSITY

### **F.1** Beckman Coulter SA 3100 [9]

The SA 3100 surface area and pore size analyzer use the principle described in section 4.7. It is operated by the department of chemical engineering at NTNU.

Helium is used to measure the free-space of the specimen which is put in a test tube. After hydrogen is helium the gas with highest permeability through a solid. The machine provides highly accurate data.



Figure F.1.: Beckman Coulter SA 3100

## BIBLIOGRAPHY

- [1] Yunus A. Çengel. *Heat and Mass Transfer - A Practical Approach (Third Edition)*. McGraw Hill, 2006.
- [2] Targets for Onboard Hydrogen Storage Systems for Light-Duty Vehicles. Technical Report Revision 4.0, U.S. Department of Energy, September 2009.
- [3] Richard J. Goldstein Ernst R. G. Eckert. *Measurement in Heat Transfer (Second Edition)*. Springer-Verlag, 1970.
- [4] James Joosten et. al. The Impact of Increased Use of Hydrogen on Petroleum Consumption and Carbon Dioxide Emissions. Technical Report SR-OIAF-CNEAF/2008-04, U.S. Energy Information Administration, August 2008.
- [5] M. Lamvik. Thermal Conductivity of Ocean Sediments. Technical report, The University of Trondheim, The Norwegian Institute of Technology Division of Thermodynamics, October 1991.
- [6] Hugo Ryvik. Drivstoff i fremtiden - Fri oss fra eksosen. *HORISONT*, 3, 2006.
- [7] Stephen Whitaker. Flow in Porous Media 1: A Theroretical Deviation of Darcy's Law. *Transport in Porous Media*, 1986.

## EQUIPMENT AND MATERIAL REFERENCES

- [8] Material Properties of Al, Matweb. <http://www.matweb.com/search/DataSheet.aspx?MatGUID=0cd1edf33ac145ee93a0aa6fc666c0e0>, December 2009.
- [9] SA 3100 Surface Area and Pore Size Analyzer, Beckman Coulter. [http://www.beckmancoulter.com/coultercounter/product\\_SA3100.jsp](http://www.beckmancoulter.com/coultercounter/product_SA3100.jsp), December 2009.
- [10] Material Properties of Cu, Matweb. <http://www.matweb.com/search/DataSheet.aspx?MatGUID=ca486cc7cefa44d98ee67d2f5eb7d21f>, December 2009.
- [11] Systronik P2601, Elma Instruments. [http://www.elma-instruments.no/\\_nb-NO/v:2278;250?visma5.prodno=5706445570355](http://www.elma-instruments.no/_nb-NO/v:2278;250?visma5.prodno=5706445570355), December 2009.
- [12] Micanite Flat Heating Element, Friedr Freek. <http://www.freek-heaters.com/products/flatheatingelements.php>, December 2009.
- [13] Flo-Rite Series FR Flowmeters, Key Instruments. <http://docs-europe.electrocomponents.com/webdocs/062b/0900766b8062b857.pdf>, December 2009.
- [14] 45W Laboratoriestrømforsyning 0-30VDC justerbar, Mascot. <http://altitec.no/strmforsyninger/45w-laboratoriestrmforsyning-030vdc-justerbar.html>, December 2009.
- [15] Manteltermoelementer, Max Siervert AS. <http://www.maxsievert.no/accounts/432765/File/G3/1182.pdf>, November 2009.
- [16] Mettler AT261, Mettler Toledo. [http://www.ietltd.com/pdf\\_datasheets/AT261\%20Data\%20Sheet.pdf](http://www.ietltd.com/pdf_datasheets/AT261\%20Data\%20Sheet.pdf), December 2009.
- [17] USB Single Module Carrier, National Instruments. <http://sine.ni.com/nips/cds/view/p/lang/en/nid/204178>, December 2009.
- [18] Thermocouple Input Module, National Instruments. <http://sine.ni.com/nips/cds/view/p/lang/en/nid/14165>, December 2009.
- [19] Filter-Regulator and Lubricator, Nordgren. <http://docs-europe.electrocomponents.com/webdocs/007a/0900766b8007a030.pdf>, December 2009.
- [20] Proportional Pressure Control Valve, Nordgren. <http://docs-europe.electrocomponents.com/webdocs/0088/0900766b80088543.pdf>, December 2009.
- [21] Cartridge heater, Omega. [http://www.omega.com/ppt/pptsc.asp?ref=CIR\\_14&Nav=head01](http://www.omega.com/ppt/pptsc.asp?ref=CIR_14&Nav=head01), December 2009.
- [22] Material Properties of PFTE, Erling Klinger Kunststofftechnik. [http://www.elringklinger-kunststoff.de/pages/e\\_werkst\\_elring\\_ptfe.html](http://www.elringklinger-kunststoff.de/pages/e_werkst_elring_ptfe.html), December 2009.

- [23] Thermocouple Application Note, Pico Technology. <http://www.picotech.com/applications/thermocouple.html>, November 2009.
- [24] Material Properties of PMMA, Matbase. <http://www.matbase.com/material/polymers/commodity/pmma/properties>, December 2009.
- [25] Material Properties of Styrofoam HD300, DOW Building Resources. [http://building.dow.com/ap/in/prod/styro\\_hd300.htm](http://building.dow.com/ap/in/prod/styro_hd300.htm), December 2009.
- [26] Thermogravimetric Analyser Q500, TA Instruments. <http://www.tainstruments.com/product.aspx?id=20&n=1&siteid=11>, December 2009.